



Short-term response of *Emiliana huxleyi* growth and morphology to abrupt salinity stress

Rosie M. Sheward¹, Christina Gebühr^{1,2}, Jörg Bollmann³, Jens O. Herrle^{1,2}

¹Institute of Geosciences, Goethe-University Frankfurt, Frankfurt am Main, D-60438, Germany

5 ²Biodiversity and Climate Research Centre (BIK-F), Frankfurt am Main, D-60325, Germany

³Department of Earth Sciences, University of Toronto, Toronto, M5S3B1, Canada

Correspondence to: Rosie M. Sheward (sheward@em.uni-frankfurt.de)

Abstract. The marine coccolithophore species *Emiliana huxleyi* tolerates a broad range of salinity conditions over its near-
10 global distribution, including the relatively stable physiochemical conditions of open ocean environments and nearshore
environments with dynamic and extreme short-term salinity fluctuations. Previous studies show that salinity impacts the
physiology and morphology of *E. huxleyi*, suggesting that salinity stress influences the calcification of this globally important
species. However, it remains unclear how rapidly *E. huxleyi* responds to salinity changes and therefore whether *E. huxleyi*
15 morphology is sensitive to short-term, transient salinity events (such as occur on meteorological timescales) in addition longer
duration salinity changes. Here, we investigate the real-time growth and calcification response of two *E. huxleyi* strains isolated
from shelf-sea environments to the abrupt onset of hyposaline and hypersaline conditions over a time periods of 156 h (6.5
days). Morphological responses in the size of the cellular exoskeleton (coccosphere) and the calcium carbonate plates
(coccoliths) that form the coccosphere occurred as rapidly as 24-48 h following the abrupt onset of salinity 25 (hyposaline)
and salinity 45 (hypersaline) conditions. Generally, cells tended towards smaller coccospheres (-24%) with smaller coccoliths
20 (-7 to -11%) and reduced calcification under hyposaline conditions whereas cells growing under hypersaline conditions had
either relatively stable coccosphere and coccolith sizes (Mediterranean strain RCC1232) or larger coccospheres (+35%) with
larger coccoliths (+13%) and increased calcification (Norwegian strain PLYB11). This short-term response is consistent with
reported coccolith size trends with salinity over longer durations of low and high salinity exposure in culture and under natural
salinity gradients. The coccosphere size response of PLYB11 to salinity stress was greater in magnitude than observed in
25 RCC1232 but occurred after a longer duration of exposure (ca. 96-128 h) to the new salinity conditions compared to RCC1232.
In both strains, coccosphere size changes were larger and occurred more rapidly than changes in coccolith size, which tended
to occur more gradually over the course of the experiments. Variability in the magnitude and timing of rapid morphological
responses to short-term salinity stress between these two strains supports previous suggestions that the response of *E. huxleyi*
to salinity stress is strain specific. At the start of the experiments, the light condition was also switched from a light: dark cycle
30 to continuous light with the aim of desynchronising cell division. As cell density and mean cell size data sampled every 4 h
showed regular periodicity under all salinity conditions, the cell division cycle retained its entrainment to pre-experiment light:
dark conditions for the entire experiment duration. Extended acclimation periods to continuous light are therefore advisable



for *E. huxleyi* to ensure successful desynchronisation of the cell division cycle. When working with phased or synchronised populations, data should be compared between samples taken from the same phase of the cell division cycle to avoid artificially
35 distorting the magnitude or even direction of physiological or (bio)geochemical response to the environmental stressor.

1 Introduction

Shifts in ocean salinity are an indirect effect of climate change, reflecting changes in the hydrological cycle on seasonal to multi-annual timescales (precipitation, evaporation, and river runoff) and dynamics in ocean circulation patterns and the cryosphere on seasonal to multi-decadal timescales (e.g. Durack et al., 2012; Westra et al., 2014; Haumann et al., 2016;
40 Lenderink and Van Meijgaard, 2008; Yu et al., 2021). Observational records indicate that open-ocean regions of higher salinity have become increasingly saline whilst regions of lower salinity have become fresher, enhancing sub-surface salinity in the subtropics and freshening the tropics and sub-polar/polar regions (Durack and Wijffels, 2010; Fox-Kemper et al., 2021). Salinity in coastal areas, continental shelf-seas, marginal seas and (semi-) enclosed basins naturally fluctuates on daily to
45 decadal timescales and salinity trends are more localised and complex, related to a combination of meteorological events, climate-driven changes in the hydrological cycle, and the impact of other local anthropogenic stressors (e.g. land use, vegetation cover, and water management pressures). Recent and future salinity trends for coastal areas, marginal seas and (semi-) enclosed basins remain uncertain, but modelling indicates, for example, that UK shelf seas will freshen in future (Dye et al., 2020).

Salinity is a major abiotic factor influencing marine ecosystem structure and function but the impact of salinity on marine
50 organisms has received relatively little attention compared to other climate-related environmental stressors (e.g., Röthig et al., 2023) and references therein). Salinity stress triggers a range of metabolic responses, including internal osmotic and ionic adjustments that can lead to morphological changes, changes to photosynthesis and respiration rates, and biochemical changes such as to osmolyte synthesis (e.g., Kirst, 1990). The response of marine phytoplankton to salinity stress has largely been investigated in coastal and euryhaline species that naturally experience variable salinity conditions, including extreme and/or
55 short-lived salinity events. For example, at one station on the French Atlantic coast, the typical winter salinity range was 5 to 35 with on average four short-lived extreme low salinity events (transient salinity decreases of ca. 2 to >20) each year lasting from a few days to a few weeks (Poppeschi et al., 2021). In the open ocean, extreme salinity anomalies are more typically defined by shifts of 0.2 to 1 pss associated with freshening events, the transit of mesoscale eddies, and atmosphere-ocean dynamics related to El Niño Southern Oscillation, Madden-Julian Oscillation and North Atlantic Oscillation (Liu et al., 2023).
60 Additionally, tropical cyclones can shift salinity by as much as 6 pss for days to weeks (Xu et al., 2020a). Both coastal and open ocean phytoplankton species therefore experience varying degrees of salinity change over a range of short- and long-term timescales. Laboratory experiments indicate that some marine phytoplankton species are broadly tolerant to salinity change whilst others are not, suggesting that the impact of salinity on phytoplankton physiology may be strain-specific (e.g. Brand, 1984).



65 One marine phytoplankton species with a demonstrated broad salinity tolerance is the coccolithophore *Emiliana huxleyi*,
which can grow under salinities as low as ca. 11-15 (Brand, 1984; Paasche et al., 1996; Lohbeck et al., 2013) and as high as
ca. 38-45 (Bukry, 1974; Brand, 1984; Winter et al., 1979; Fisher and Honjo, 1988; Gebühr et al., 2021; Linge Johnsen et al.,
2019; Fielding et al., 2009). *E. huxleyi* has a near-global open ocean distribution (limited presence or absence the very high
latitudes (e.g., Winter et al., 2013) but also thrives in the shelf-seas and coastal environments. For example, large blooms of
70 *E. huxleyi* are observed in Norwegian coastal waters and fjords in the summer (e.g. Holligan et al., 1993; Van Der Wal et al.,
1995; Winter et al., 2013) in addition to shelf-sea blooms and blooms in the open ocean (e.g., Poulton et al., 2013; Tyrrell and
Merico, 2004; Poulton et al., 2014).

Previous studies have demonstrated that the physiological response of coccolithophores to changing environmental conditions
can influence the size of the individual plates (coccoliths) that form the coccolithophore exoskeleton (the coccosphere) (e.g.,
75 Faucher et al., 2020; Bollmann, 1997; Bollmann and Herrle, 2007). Laboratory experiments show that hyper- and hyposaline
conditions impact the growth and morphology of many *E. huxleyi* strains (Saruwatari et al., 2016; Green et al., 1998; Paasche
et al., 1996; Linge Johnsen et al., 2019; Xu et al., 2020b; Gebühr et al., 2021). Additionally, coccolith size varies systematically
along natural sea surface salinity gradients (Bollmann and Herrle, 2007; Bollmann et al., 2009). In light of this morphological
sensitivity to salinity conditions, a transfer function relating *E. huxleyi* coccolith size and salinity has been developed to derive
80 paleo-salinity records independently of other geochemical proxies for use in paleoclimate and paleoceanography research
(Herrle et al., 2018; Bollmann et al., 2009; Bollmann and Herrle, 2007). Cellular osmotic adjustments that change cell size
have been proposed as the driver of the observed morphological response of *E. huxleyi* coccoliths to salinity stress (Bollmann
et al., 2009; Gebühr et al., 2021) but the mechanistic link between salinity and cellular morphology remains unclear. Another
open question is how rapidly *E. huxleyi* growth and morphology can respond to salinity changes, which could range from small
85 salinity fluctuations (up to ca. 1; e.g., Liu et al., 2023) over seasonal to annual timescales in the open ocean to large magnitude
salinity events (decreases of up to ca. 5-20; e.g., Poppeschi et al., 2021) with a rapid onset and short duration in coastal
environments.

The aim of this study was to observe the short-term response of *E. huxleyi* growth, morphology, and calcification to an abrupt
exposure to low and high salinity conditions by taking measurements for cell concentrations, coccosphere size and coccolith
90 size every ca. 4 h for 6.5 days. Cultures were simultaneously transitioned from a light: dark cycle to continuous light at the
onset of the salinity treatment with the aim that continuous light conditions would desynchronise the cell division cycle by the
end of the experiment. Whilst our sampling frequency aimed to identify how quickly morphology responded to salinity stress,
an unintended advantage of our 4 h sampling regime was the real time observation of the response of the cell division cycle to
both salinity stress and the onset of continuous light conditions.



95 2 Methods

2.1 *Emiliana huxleyi* cultures

The *E. huxleyi* strain PLYB11 (Plymouth Culture Collection, UK) is an isolate from the coastline near Bergen, Norway, with a natural seasonal salinity range of ca. 25-34 (Paulino et al., 2018). Strain RCC1232 (Roscoff Culture Collection, France) is a coastal isolate from the Bay of Villefranche-sur-Mer, France. The salinity range in this region of the northwest Mediterranean Sea is ca. 37-38 (Kapsenberg et al., 2017). Stock cultures of both strains were maintained at 15 °C under 12 h light: 12 h dark conditions at an irradiance of ca. 70 $\mu\text{mol photons m}^{-2} \text{s}^{-1}$ and salinity of 35. Cultures were grown in sterile *f*/2-enriched artificial seawater prepared using a commercial sea salt mixture (Ultramarine, Waterlife Research Industries Ltd., UK) that was dissolved in Milli-Q water with the addition of 0.5 g L⁻¹ Tricine to prevent salt precipitation during autoclaving.

2.2 Salinity experiments

105 Cultures of PLYB11 and RCC1232 were grown under three salinity conditions: 25 (low salinity/hyposaline treatment), 35 (control), and 45 (high salinity/hypersaline treatment). The *f*/2-enriched artificial seawater described above was diluted to the final experimental salinity by the addition of sterilised Milli-Q. To initiate each salinity experiment, triplicate 70 mL polycarbonate flasks with vented lids were prepared with 60 mL of sterile salinity 25, 35, or 45 media and directly inoculated with a small volume of stock culture (35 salinity) to achieve a start concentration of ca. 2×10^5 cells mL⁻¹. Culture flasks were sampled continuously every four hours from the start of the experiment (0 h at 22:00 local time for PLYB11 and 00:00 local time for RCC1232) for 6.5 days (156 h) so that high resolution temporal data could be collected to monitor how rapidly growth and morphology responded to the abrupt change in salinity conditions. At the end of the light phase preceding the start of the experiment (06:00 h to 18:00 h local time), light in the experimental incubator was left on continuously for the duration of the experiment, thereby switching the experimental cultures from a 12 h light, 12 h dark regime to a continuous light regime at 0 h. Continuous light conditions are often used to desynchronise the cell cycle (e.g., Müller et al., 2008, 2015) and with our 4 h measurement frequency, we were able to additionally track how long the cell division cycle remained entrained to the previous 12:12 light/dark regime by analysing changes in cell concentrations and cell size through the experiments.

2.3 Cell concentration and growth

At each sampling time point, flasks were gently mixed to ensure the homogenous suspension of cells throughout the seawater before sampling and to re-equilibrate air in the flask headspace with sterile air. The sampling timepoints for cell concentration for PLYB11 were 22:00 h, 02:00 h, 06:00 h, 10:00 h, 14:00 h and 18:00 h local time. For strain RCC1232, the sampling timepoints were 00:00 h, 04:00 h, 08:00 h, 12:00 h, 16:00 h, 20:00 h local time. The cell concentration data at 10:00 h (PLYB11) and 12:00 h (RCC1232) local time (7 of a total of 40 sampling timepoints for each experiment, selected to represent a 24 h sampling frequency) have been previously presented in Gebühr et al. (2021).



125 Cell concentration was determined from a 400 μL aliquot of culture (dilution factor of 26) using an automatic cell counter
(CASY Model TT, OMNI Life Science). Cell concentrations are reported as viable cells measured between 3.00 to 20.03 μm
using a 60 μm capillary, the lower cell size threshold having been determined for these strains prior to the start of the
experiment. The CASY cell counter also reports particle (cell) size distribution in the sample and here we report cell size from
CASY derived at 4 h time intervals from the mean volume measured between 3.00 to 20.03 μm on the same aliquot. Cell
130 volume measurements from CASY have a maximum error of $\pm 2\%$ (OMNI Life Science).

Daily growth rates $\mu_{24\text{h}}$ (d^{-1}) were calculated from cell concentration data following Eq. (1):

$$\mu_{24\text{h}} = \frac{\ln N_t - \ln N_{t-24\text{h}}}{t - t_{-24\text{h}}} \quad (1)$$

where $N_{t-24\text{h}}$ and N_t are the cell concentration, N , of the culture at two sampling time points, t and $t_{-24\text{h}}$, that are consecutive
but separated by 24 h, e.g. sampling at 10pm or at 2pm on two consecutive days (Guillard, 1973; Wood et al., 2005).

135 Instantaneous cell division rates μ_t (h^{-1}) were calculated for overlapping 8 h time intervals following Eq. (2) (Nelson and
Brand, 1979):

$$\mu_t = \frac{1}{N_t} \frac{N_{t+4\text{h}} - N_{t-4\text{h}}}{8\text{h}} \quad (2)$$

2.4 Coccolith and coccosphere morphometrics

Samples for measurement of coccosphere diameter (size including the external layer(s) of coccoliths, \emptyset) and coccolith length
140 (C_L) using scanning electron microscopy (SEM) were taken ca. every 8 hours beginning at 12 h. At each sampling timepoint,
2 to 5 mL of culture from each flask were gently filtered on a polycarbonate filter (0.8 μm pore size, 25 mm diameter) using a
borosilicate vacuum filtration flask (Millipore) and air dried for 24 h. For each salinity treatment, one of these triplicate filters
was then mounted onto an aluminium stub and sputter-coated with 4-nm platinum for SEM imaging using a field-emission
SEM (Zeiss SIGMA VP). Measurements at 0 h were taken from a single filter from the salinity 35 stock culture used to
145 inoculate each experimental flask (i.e., the size measurements at 0 h are the same for all salinity experiments for each strain).
Coccolith size measurements were made for a minimum of 50 flat-lying, individual coccoliths at a magnification of 20,000x
from each filter and at least 50 intact coccospheres were imaged at a magnification of 10,000x for coccosphere size
measurements. Measurements were made using ImageJ (v.1.51) from images with a dimension of 1024 x 768 pixels. Coccolith
and coccosphere size measurements were calibrated to 2 μm polystyrene calibration beads (certified mean diameter 1.998 μm
150 ± 0.016 μm ; Duke Standards Microsphere 4000 Series, certified batch number 4202–008) filtered onto a polycarbonate filter
and measured once vertically and once horizontally then averaged. Coccosphere size was similarly measured as the average
of one vertical and one horizontal measurement (Lamoureux and Bollmann, 2004; Nederbragt et al., 2004).

Measurements of \emptyset , C_L and coccolith width from a single sampling timepoint on experiment day 7 (timepoint 14.07.2014
10:00 h for PLYB11, all salinities) and at a single sampling timepoint on experiment day 5 (12.07.2014 12:00 h salinity 25
155 and 35) or day 7 (13.07.2014 20:00 h salinity 45) for RCC1232 have previously been presented in Gebühr et al. (2021).
Morphometric data for the other ca. 18 sampling timepoints in each experiment is presented here for the first time.



2.5 Cellular calcite and biomass

To further quantify the impact of morphometric responses to short-term salinity stress on calcification and cellular biogeochemical traits of *E. huxleyi*, we estimated cellular calcite content (particulate inorganic carbon content, PIC), biomass
160 (particulate organic carbon content, POC) and the calcite:biomass ratio (PIC:POC) of both strains towards the end of each salinity experiment. Cellular calcite (PIC) was estimated following the method of Young and Ziveri (2000), where cell calcite is a function of C_L and the number of coccoliths per coccosphere (C_N) following Eq. (3):

$$\text{cellular calcite, PIC (pg cell}^{-1}\text{)} = (C_L^3 \times 2.7 \times K_s) \times C_N \quad (3)$$

where K_s is a shape factor that describes species-specific coccolith morphology and 2.7 is the density of calcite ($\text{pg } \mu\text{m}^{-3}$).
165 Various K_s values have been published for *E. huxleyi* but here we use K_s values published by Linge Johnsen et al. (2019) that are specific to strain PLYB11 ($K_s = 0.014\text{-}0.015$) and strain RCC1232 ($K_s = 0.017\text{-}0.019$) and derived from experiments using the same salinity conditions as applied here. Within sample 148 h (PLYB11) and 140 h (RCC1232) from each salinity experiment, the C_N of 30 individual coccospheres (the number of coccoliths visible on each coccosphere surface multiplied by two to approximate total number of coccoliths per coccosphere) and the C_L of one of the coccoliths present on the surface of
170 the same coccospheres (i.e., distinct from the C_L measured on exclusively loose, flat-lying coccoliths) were measured from each SEM image to estimate cell-specific PIC using Eq. 1.

Cellular biomass (POC) was estimated as a function of cell volume. Cell diameter cannot be directly measured from SEM images (as the coccosphere obscures the internal organic biomass) and was therefore estimated for the same 30 coccospheres in 148 h and 140 h samples of both strains by subtracting 2x coccolith thickness (using mean coccolith thickness values for
175 PLYB11 and RC1232 at salinity 25, 35 and 45 conditions from Linge Johnsen et al., 2019) from our measurements of coccosphere diameter for each cell. Cell POC was then estimated following Eq. 4 (Menden-Deuer and Lessard (2000) for prymnesiophytes):

$$\text{cellular biomass, POC (pg cell}^{-1}\text{)} = 0.23(\text{cell volume})^{0.9} \quad (4)$$

2.6 Media chemistry

180 The pH and total alkalinity were measured at the beginning (0 h) and end (156 h) of each salinity experiment. A portable pH meter (WTW Multi 3400i, Xylem Analytics, Germany) was used to measure pH and a titration method (MQuant Alkalinity Test, Merck) was used to measure alkalinity. Dissolved inorganic carbon (DIC) was calculated approximately as the difference between the two acid capacity values determined through titration ($K_{S4.3} - K_{S8.2}$).

2.7 Statistical analysis and data visualisation

185 Statistical analysis was performed using GraphPad Prism for macOS (v8.4.1, GraphPad Software, LLC). A one-way ANOVA was performed to assess statistical changes in coccolith size or coccosphere diameter through time within each salinity experiment with a Tukey's post-hoc test to identify the source of the main effect determined by ANOVA. Data were considered



significant at the 95% confidence interval ($p < 0.05$). Data figures were plotted in GraphPad Prism and final layout was arranged using Adobe Illustrator.

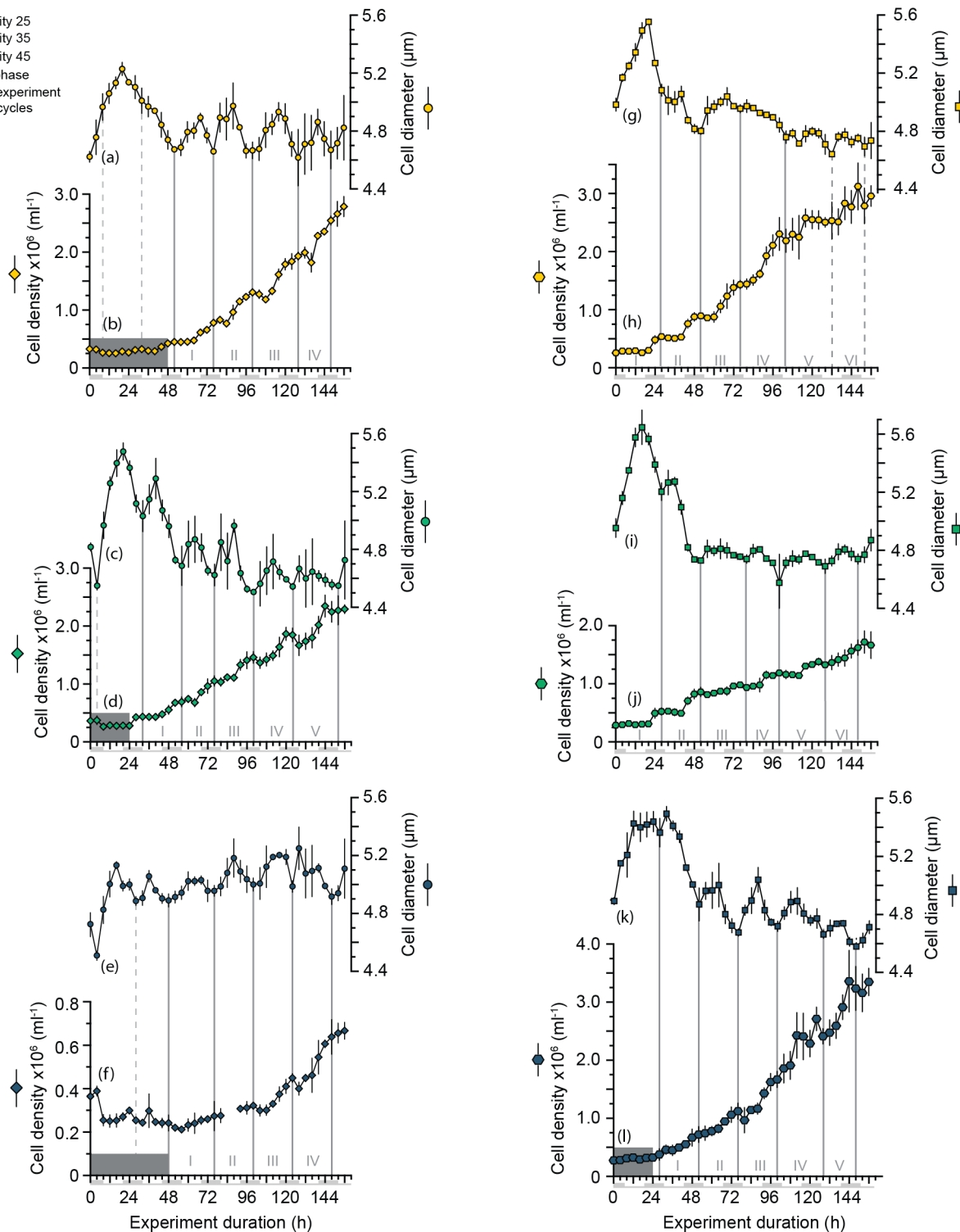
190 3 Results

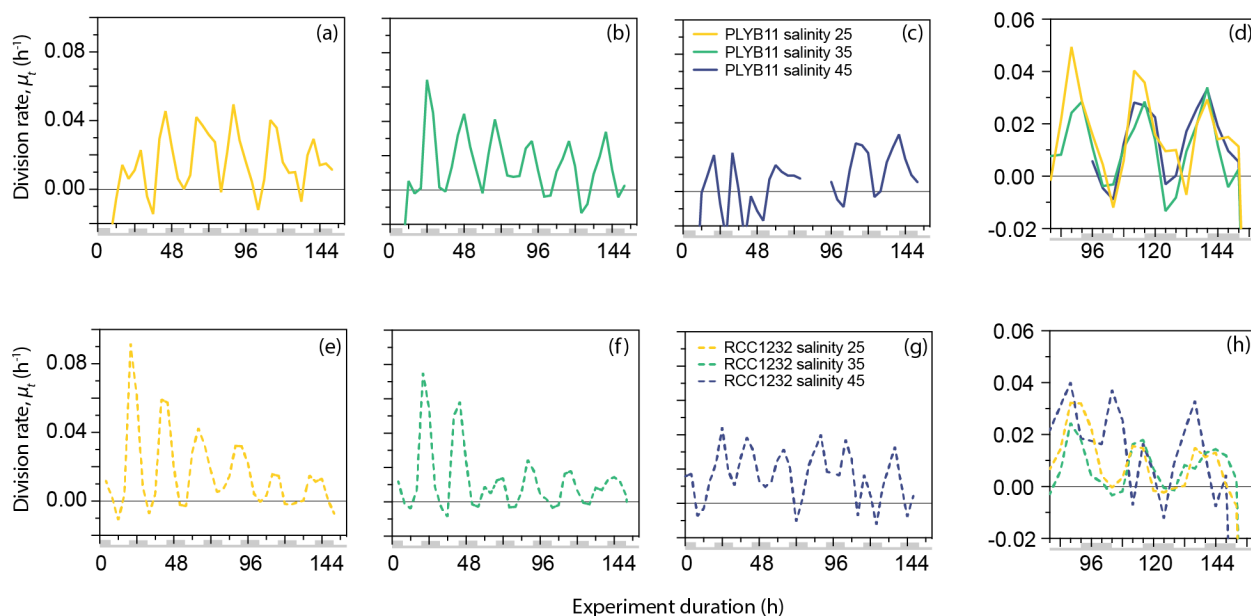
3.1 Cell division phasing and growth under three salinity conditions

Under all salinity conditions, the mean cell size and cell concentration of *E. huxleyi* PLYB11 cultures during the experiments (Fig. 1a-f) shows a repeating cyclicality that represents a phased cell division cycle, i.e., a portion of (but not all) cells in the culture are moving collectively through the cell division cycle each 24 h period (see also Chisholm (1981) for terminology).
195 This cell division cycle phasing persisted for the complete duration of the experiment (6.5 d) after the onset of continuous light conditions (at 0 h, previously acclimated to 12:12 L:D) under all salinity conditions. Phasing of the cell division cycle was identified by distinct maxima and minima in mean cell diameter that were repeated with an interval of $24 \text{ h} \pm 4 \text{ h}$ as well as regular intervals of increasing cell concentration (indicating an interval of population division) followed by a plateau in cell concentration (indicating an interval of production, or no cell division). Intervals of increasing cell concentration aligned with
200 the occurrence of cell size minima, as would be expected during an interval of phased cell division. Under all salinity conditions, consecutive cell size minima and periods of increasing cell concentration occurred during what would have been the last 4-8 h of the pre-experiment dark period (indicated by the alternating grey shading within the x-axis of Fig. 1). Cyclical fluctuations in cell concentrations and cell diameter were also apparent in strain RCC1232 under all salinities (Fig. 1g-l). However, intervals of cell concentration increase/stasis and shifts from cell size minima to cell size maxima were less
205 uniform and there was typically a smaller size change between successive cell diameter minima and maxima in this strain compared to PLYB11. Cell diameter fluctuations in RCC1232 were most pronounced under salinity 45 (Fig. 2k). Mean cell diameter minima tended to occur every 24 to 28 h under all salinity conditions, with longer intervals between cell diameter minima occurring after ca. 72 h of the experiment. Intervals of minimum cell diameter typically coincided with the end of an interval of increasing cell concentration, comparable to the observations for PLYB11.

210

Figure 1: Cell density and cell diameter of *E. huxleyi* strains PLYB11 (a-f) and RCC1232 (g-l) over the 156-h duration of experiments under salinity 25 (hyposaline), salinity 35 (control) and salinity 45 (hypersaline) conditions. Each data point represents the mean and standard deviation of triplicate measurements. Note the different y-axis scale in (f). Sequential population division cycles are indicated by the vertical grey lines and numbered with Roman numerals, determined by mean cell diameter minima. Some experiments exhibit a period of minimal growth or an initial lag phase in the first 24-48 h, indicated by the dark grey shaded area. Inferred division cycles that occur during these initial lag phases are denoted by dashed grey lines. For context, the timing of pre-experiment alternations between light and dark (L:D) conditions are shown as light grey shading within the x-axis labels (note that continuous light conditions were applied for the duration of all
215
220 experiments; see Methods).





225

Figure 2: Division rates, μ_t , of *E. huxleyi* strains PLYB11 (a-d) and RCC1232 (e-h) over the duration of experiments under salinity 25 (hyposaline), salinity 35 (control) and salinity 45 (hypersaline) conditions. For comparison across the three salinity treatments, division rates over days 4-6.5 of the experiments are shown in (d) for PLYB11 and (h) for RCC1232 (note the different y-axis scale). Similarly to Fig. 1, the timing of pre-experiment alternations between light and dark conditions are shown as light grey shading within the x-axis labels for context.

230

The 156-h duration of the experiments represented just over six division-production cycles during which approximately one third to one half of the population moved through cell division (growth rates, μ_{24h} , ranging from 0.26 d⁻¹ in PLYB11 under salinity 45 to 0.41 d⁻¹ in RCC1232 under salinity 45). The experiment duration therefore represented between 2 and 4 complete generations under the salinity conditions. Instantaneous cell division rates (μ_t , 8 h averaging) fluctuated between a minimum of ca. -0.01 h⁻¹ and 0.02-0.049 h⁻¹ at salinity 25, 0.03-0.064 h⁻¹ at salinity 35, and ca. 0.015-0.033 h⁻¹ at salinity 45 for PLYB11 (Fig. 2a-c), with an interval of 24 h ± 4 h between peak division rates throughout the experiments. For RCC1232, instantaneous cell division rates (Fig 2e-g) fluctuated between ca. -0.01 h⁻¹ (minimum for all salinity treatments) and 0.015-0.092 h⁻¹ at salinity 25, 0.014-0.075 h⁻¹ at salinity 35, and 0.017-0.044 at salinity 45 with an interval of 24 h ± 4 h between peak division rates. Division rate minima typically occurred during what would have been the last 4-8 h of the pre-experiment dark period or the first 4-8 h of the pre-experiment light period in both strains. In the first 48 hours, RCC1232 under salinity 25 and salinity 35 conditions shows large peak division rates that decrease by more than half by 72 h. Such a large change in peak division rates between the first 2 days and the remainder of the experiment duration is not observed in PLYB11. After 3-4 days of

235

240



growth under the experimental treatments (between 80 h and 152 h), periodicity in cell division rates clearly persists (Fig. 2d, 245 h) but peak division rates start to decline in both strains under salinity 25 and 35 by ca. 144 h in both strains (peak μ_t decreasing from ca. 0.04-0.06 h^{-1} to 0.02-0.05 h^{-1} in PLYB11 and peak μ_t decreasing from 0.025-0.035 h^{-1} to 0.01-0.015 h^{-1} in RCC1232). In days 4-6 of the salinity 45 experiment with RCC1232, a 4-8 h offset between the timing of peak division and the timing of peak division under salinity 25 and 35 also emerges (Fig. 2h). For PLYB11, peak division rates in the final 3 days of each salinity experiment all occur at the same timepoint (Fig. 2d).

250 Based on the logarithmic transformation of cell concentration data, all PLYB11 experiments (including control salinity 35) and RCC1232 salinity 45 experiment showed an initial lag phase of 24 h to 48 h. Mean cell size increased by 0.5-0.9 μm over the first ca. 12 h of each experiment before decreasing again over the following 12-24 h. This was equivalent to a mean cell size increase of 11% (RCC1232) or 13% (PLYB11) at salinity 25 and 45 and an increase of 14% (RCC1232) or 20% (PLYB11) at salinity 35 (Fig 1 and 2). In RCC1232 and PLYB11 salinity 35 and 45 experiments, the subsequent mean cell size decrease 255 was not as great as the initial size increase in the first 12-24 h of the experiment and was followed by a smaller size increase at the beginning of division cycle II (similar in magnitude to subsequent mean size minima-maxima fluctuations for the remainder of the experiment). In both strains under salinity 35, division cycle II (between 32 h and 56 h in PLYB11 and 28 h and 52 h in RCC1232) saw a large size decrease during the interval of increasing cell concentrations.

3.2 Effect of salinity on coccolith and cell size in PLYB11

260 Under control salinity 35 conditions, coccolith size (C_L) and coccosphere size (\emptyset) in PLYB11 remained relatively unchanged for the duration of the experiment, showing only minor fluctuations through time (Fig. 3b and e). Following the abrupt transition to salinity 25, mean C_L responded to the abrupt transition to salinity 25 with a significant decrease from 2.9 to 2.6 μm (-10%) within the first 12 h of exposure (one-way ANOVA, $F(7, 410)=6.493$, $p<0.0001$; Tukey post-hoc showed that C_L measured at 0 h is statistically larger than all other measured timepoints and no other multiple comparisons were statistically 265 significant; Fig. 3a) and mean C_L remained at 2.5-2.7 μm for the remainder of the salinity 25 experiment. Under salinity 45, mean C_L increased in two stages (Fig 3c), with a small but significant step increase of ca. 7% at 36 h and a further ca. 9% increase in C_L at 100 h. Mean \emptyset also changed at a similar timepoint to C_L change under salinity 45 (Fig. 3d-f), gradually increasing from 4.9 μm at 76 h to 5.3 μm at 100 h (an equivalent mean cell volume increase of 27%) after which mean \emptyset remained relatively constant at 5.1-5.3 μm (Fig 3f). In contrast, the response of mean \emptyset to salinity 25 occurred later in the 270 experiment than the response of mean C_L , decreasing from 5.0 μm to 4.5 μm between 100 h and 132 h. The mean \emptyset at the end of the salinity 25 experiment (156 h) was 4.2 μm (an equivalent cell volume decrease of 41%).

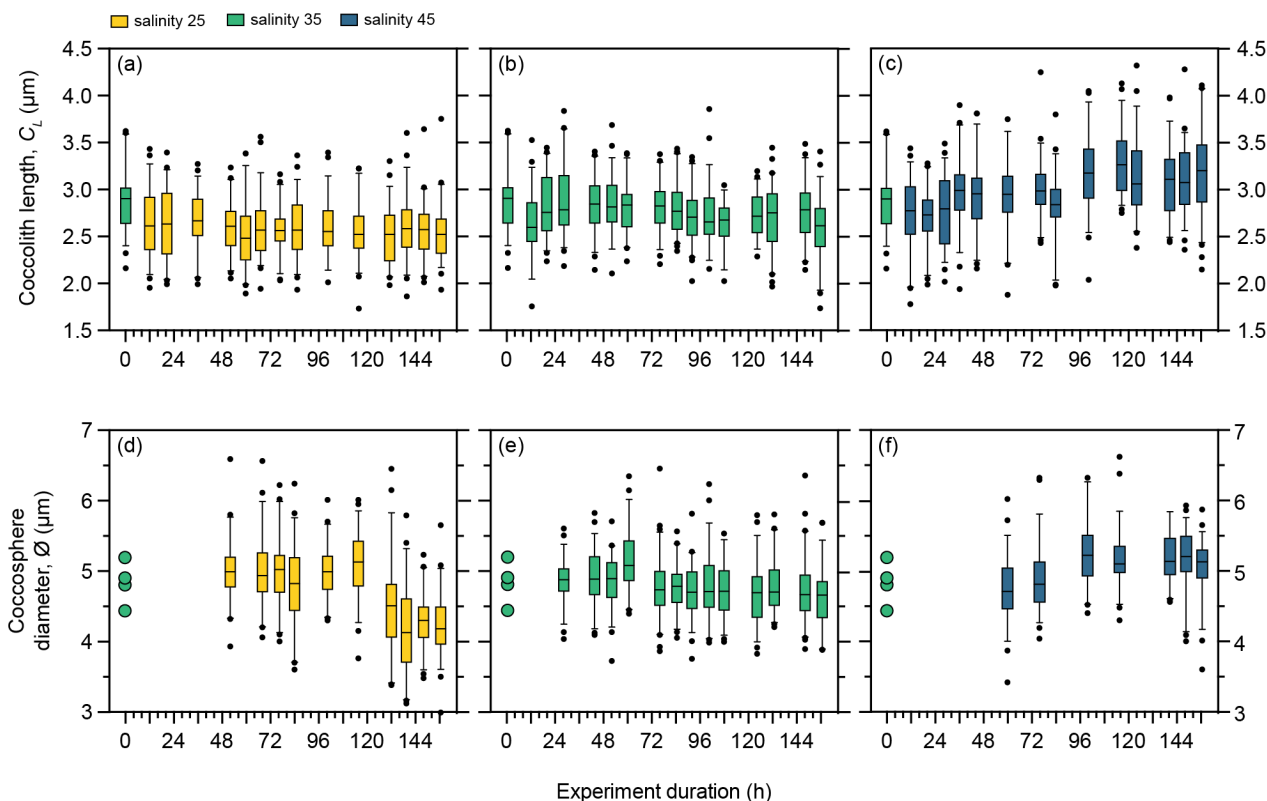


Figure 3: Morphology of *E. huxleyi* strain PLYB11 under three salinity conditions over 156 h exposure duration. (a-c) coccolith length under salinity 25, salinity 35, and salinity 45. (d-f) coccosphere diameter under salinity 25, salinity 35, and salinity 45. Box and whisker plots show the 25th-75th quartiles (box with median shown by the central line) and 5-95 quartiles (whiskers) of a minimum of 50 measurements at each timepoint. Measurements outside the 5th-95th quartiles of the data are shown as circles. Measurements at time 0 h are taken from the stock control culture (salinity 35) used to inoculate all flasks and are therefore also shown as the start coccolith length or coccosphere diameter measurements for salinity 25 and 45 experiments at 0 h. The 0 h sample for PLYB11 coccosphere diameter measurements was lost but a small number of coccosphere measurements (n=4) could be made from the coccolith length sample and are provided (circles, d-e) to indicate coccosphere diameter at 0 h in this experiment. C_L and \emptyset data at 156 h for each experiment were previously presented in Gebühr et al. (2021).

As phasing of the cell division cycle persisted under continuous light for the entire duration of the experiment, the analysis of the short-term effect of salinity on coccolith and cell size must be based on samples taken at the same timepoint within the cell cycle to avoid comparing data from later in the production phase (when cells are larger) with data from the division phase or early production phase (when cells are smaller as they have recently divided). We therefore compared temporal changes in coccolith and coccosphere size of PLYB11 under exposure to salinity 25 and 45 based on measurements taken from the same cell cycle point (cell size minima) at 76 h, 100 h, 124 h and 148 h to see if the magnitude and/or direction of salinity effects on morphology remained constant with time or changed through time as the population was exposed to the new salinity condition for longer (Fig. 4). After just three days of growth (76 h), there is a clear difference in PLYB11 C_L between low



salinity, control, and high salinity conditions, with larger C_L under higher salinity conditions (Fig. 4a). The size difference between salinity 35 and salinity 45 coccoliths becomes even more pronounced by days 4-6, i.e., with longer exposure to hypersaline conditions. By contrast, the effect of salinity on \varnothing develops more steadily as the experiment progresses (Fig. 4b): after 3-4 days growth (76 h to 100 h), coccospheres tend to be larger at salinity 25 and 45 than at salinity 35, however after 6 days of growth (148 h), mean \varnothing is smallest at salinity 25 and largest at salinity 45.

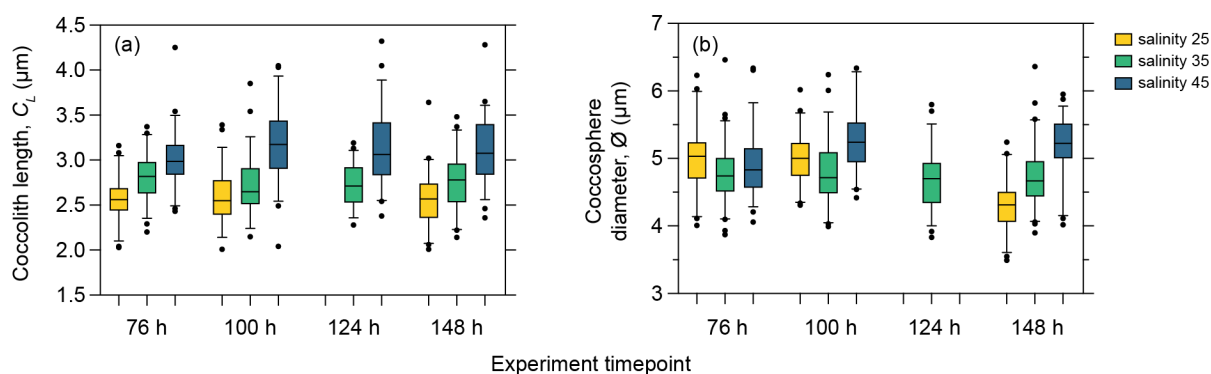


Figure 4: Coccolith length (a) and coccosphere diameter (b) response of *E. huxleyi* strain PLYB11 after 76 h (ca. 3 days), 100 h (ca. 4 days), 124 h (ca. 5 days) and 148 h (ca. 6 days) exposure to salinity 25, salinity 35 and salinity 45 conditions. The measurements from these selected timepoints are sampled from the same cell cycle timepoint (cell size minima). Samples for \varnothing were not taken at 124 h from the salinity 25 and salinity 45 experiments.

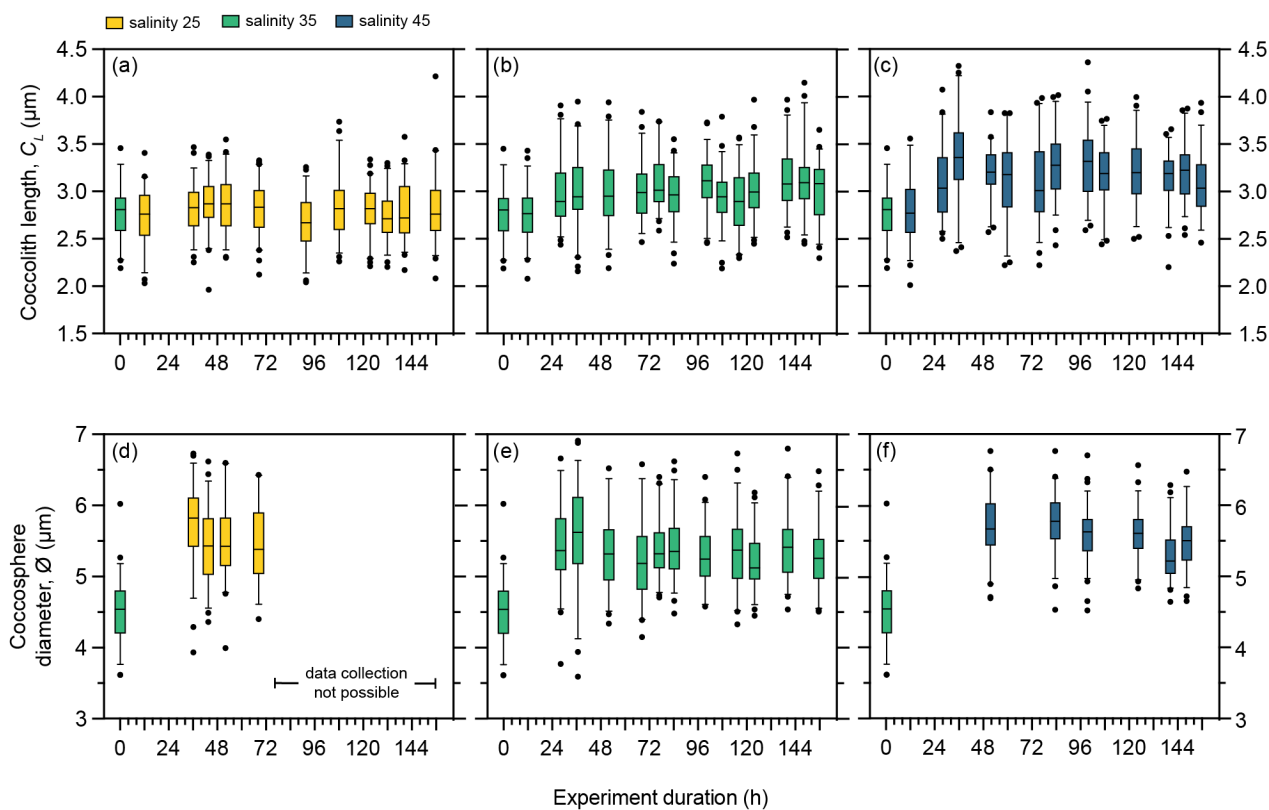
3.3 Effect of salinity on coccolith and cell size in RCC1232

In contrast to PLYB11 under control conditions, RCC1232 grown under salinity 35 showed an increase in C_L within the first 48 h (Fig. 4b; one-way ANOVA, $F(13, 744)=4.316$, $p<0.0001$; Tukey post-hoc showed that C_L measured at 12 h was significantly smaller than all other timepoints except 84 h, 108 h and 116 h and no other multiple comparisons were statistically significant). A significant increase in \varnothing within the first 24 h in the salinity 35 experiment is also clear (Fig. 4e; one-way ANOVA, $F(11, 647)=14.59$, $p<0.0001$; Tukey post-hoc showed that C_L measured at 0 h is statistically smaller than all other measured timepoints) and persisted for the remainder of the experiment (Fig 4b, e).

Mediterranean strain RCC1232 showed a negligible C_L response to salinity 25 relative to C_L at 0 h but a ca. 18% increase in C_L under salinity 45 conditions within the first 36 h of the experiment (Fig. 4a,c). A significant 28% increase in \varnothing is recorded between 0 h and 36 h under salinity 25 (Fig. 4d; Tukey multiple comparison test, $p<0.0001$, 95% C.I.=-1.550 to -0.9713). Intact coccospheres were not observed on filters after 72 h growth under low salinity. RCC1232 mean \varnothing increased by 27% over the course of the salinity 45 experiment but the \varnothing increase primarily occurred two days earlier, within the first 48 h (Fig. 4f). In the final day of the experiment, mean \varnothing under salinity 45 seems to decrease slightly.



315 To assess the overall impact of low and high salinity treatments on C_L and \emptyset , measurements from the same points of the cell
division cycle were shown for PLYB11 in Fig. 4. A comparable analysis was not possible for RCC1232 because fewer overall
SEM measurements of \emptyset were taken (and were not possible under salinity 25, as explained above) and because the timepoints
of C_L SEM measurements unfortunately did not align well with the timepoints of cell size minima/maxima as determined from
CASY data (Fig. 1g-l). However, after 3-4 days of growth under each salinity conditions, RCC1232 C_L was consistently
320 smallest under salinity 25 and largest under salinity 45 (Fig. 5). RCC1232 \emptyset under each salinity was more similar across the
different salinity conditions (based on SEM measurements; Fig. 4) but also appears to have not completely stabilised after >6
days under the new salinity conditions (based on CASY measurements; Fig. 2). Under all salinity conditions, size measured
at 0 h from the control 35 salinity inoculum was also substantially smaller than \emptyset measured at all other timepoints (Fig. 4).



325

Figure 5: Morphology of *E. huxleyi* strain RCC1232 under three salinity conditions over 156 h exposure duration. **(a-c)** coccolith length (C_L) under salinity 25, salinity 35, and salinity 45. **(d-f)** cocosphere diameter (\emptyset) under salinity 25, salinity 35, and salinity 45. Box and whisker plots show the 25th-75th quartiles (box with median shown by the central line) and 5-95 quartiles (whiskers) of a minimum of 50 measurements at each timepoint. Measurements outside the 5th-95th quartiles of the data are shown as circles. Measurements at time 0 h are taken from the stock control culture (salinity 35) used to inoculate all flasks and are therefore also shown as the start C_L or \emptyset measurements for salinity 25 and 45 experiments at 0 h. Cocosphere measurements after 96 h were not possible for the salinity 25 experiment as severe coccolith malformation led to all cocsospheres collapsing when filtered. C_L data at 108 h (salinity 25 and 35) and 140 h (salinity 45) and \emptyset data at 116 h (salinity 35) and 140 h (salinity 45) were previously presented in Gebühr et al. (2021).

330



3.4 Calcification response to salinity

335 Our short-term experiments additionally show that the rapid effect of salinity on *E. huxleyi* morphology leads to changes in
 the calcite per coccolith and calcite per cell of both strains between each salinity condition (Table 1). After ca. 6 days growth,
 the difference in the size of PLYB11 coccoliths between salinity 25 and salinity 45 conditions (+22%) in PLYB11 is equivalent
 to a 95% increase in coccolith calcite (particulate inorganic carbon, PIC) compared to PIC under salinity 25 (Table 1). In
 RCC1232, mean coccolith PIC was 26% larger under salinity 45 conditions relative to salinity 25 conditions after ca. 6 days
 340 growth but coccolith PIC was conversely largest at salinity 35, as mean C_L was only very slightly smaller at salinity 35 (>1%)
 than salinity 45 but the K_S value of RCC1232 at salinity 35 compared to salinity 45 is slightly larger (Linge Johnsen et al.,
 2019). At the cellular level, calcite per coccospere after ca. 6 days growth under salinity 45 is almost double that at salinity
 25 in PLYB11 (an increase of 1.38 pg C cell⁻¹ or 99%), principally driven by the response of C_L to salinity as the number of
 coccoliths per cell (C_N) remains relatively unchanged between salinity conditions. Cellular PIC could not be estimated for
 345 RCC1232 under salinity 25 conditions as coccospere were too poorly preserved. Cellular PIC was 4% larger under salinity
 45 compared to salinity 35 in RCC1232 after ca. 6 days growth. Larger coccospere (cell) size with increased salinity
 additionally translates to increased biomass (particulate organic carbon, POC) per cell. The interaction between increased C_L
 and \emptyset with salinity and variability in C_N between individual coccospere results in smaller differences in cellular PIC:POC
 between salinity treatments, although PIC:POC is slightly higher (ca. 8%) under salinity 45 conditions.

350

Table 1. Mean (\pm sd) values for morphology and biogeochemical parameters of *E. huxleyi* after ca. 6 days growth under three salinity
 conditions. Growth rate (μ_{24h}) is calculated between experiment day 2 and day 5 (see Methods). Morphometric data are from 148 h for
 PLYB11 and 140 h for RCC1232 (i.e., from comparable points of the cell division cycle, approximately a minimum in mean cell size).
 Coccolith length (C_L) and coccospere diameter (\emptyset) are directly measured from SEM images for a minimum of 50 individuals. See Methods
 355 for the calculation of calcification (particulate inorganic carbon, PIC) following (Young and Ziveri, 2000) and biomass (particulate organic
 carbon, POC) following (Menden-Deuer and Lessard, 2000) based on morphometric measurements from 30 individual coccospere per
 sample.

	C_L (μ m)	\emptyset (μ m)	Calcite, PIC (pg C)		Biomass, POC (pg C cell ⁻¹)	PIC:POC (mol:mol)
			per coccolith	per coccospere		
PLYB11						
Salinity 25	2.54 (0.30)	4.30 (0.39)	0.077 (0.03)	1.40 (0.43)	6.14 (1.79)	0.25 (0.10)
Salinity 35	2.76 (0.31)	4.71 (0.45)	0.110 (0.035)	1.95 (0.72)	8.00 (2.64)	0.25 (0.06)
Salinity 45	3.11 (0.36)	5.20 (0.43)	0.150 (0.054)	2.78 (0.74)	9.54 (1.93)	0.27 (0.05)
RCC1232						
Salinity 25	2.79 (0.31)	-	0.138 (0.22)	-	-	-
Salinity 35	3.11 (0.32)	5.41 (0.45)	0.191 (0.06)	3.28 (1.06)	11.84 (3.18)	0.30 (0.09)
Salinity 45	3.14 (0.29)	5.30 (0.37)	0.174 (0.04)	3.40 (1.07)	11.04 (2.28)	0.32 (0.10)



360 4 Discussion

4.1 Persistent phased cell division under continuous light

Many phytoplankton exhibit cell division cycles that are synchronised (with the population doubling each day) or phased (where population doubling time exceeds one day) to external light: dark fluctuations (Chisholm and Brand (1981) and references therein). Populations entrained to the light: dark cycle typically restrict cell division to a portion of the light: dark cycle (e.g., Nelson and Brand, 1979), usually the dark phase, and production occurs during the light phase (Harding et al., 1981). Cell division in *E. huxleyi* occurs primarily during the dark phase (Bucciarelli et al., 2007; Müller et al., 2008) under a range of light: dark conditions (Paasche, 1967). This phased cell division leads to diel variability in parameters that are commonly measured to track physiological responses to changing environmental conditions (Kottmeier et al., 2020), such as cellular biomass (POC). Cell concentrations through time (<24 h measurement frequency) will similarly show steplike increases (Kottmeier et al. 2020) when population division is phased rather than the constant exponential increase in cell concentrations expected for fully desynchronised populations (Müller et al., 2015). When sampling a phased population over a period of time, measurement timepoints therefore need to be carefully selected so that they target the same point of the cell division cycle each 24 h period (Barcelos E Ramos et al., 2010; Kottmeier et al., 2020). This is particularly important when aiming to quantify the impact of environmental perturbations on cell physiology, as absolute increases or decreases in cellular elemental content will vary throughout the day and comparing data collected from different timepoints in the cell division cycle across experiments could change the conclusions of the experiment (Kottmeier et al., 2020).

To circumvent this complexity, some experimental designs apply continuous 24 h light to cultures with the aim to fully desynchronise the cell division cycle. For a fully desynchronised population growing under continuous light, the sampling time has no influence on measurement values as all measurement timepoints are representative of the daily mean production rate, cellular elemental content or other physiological measure of interest (Jochem and Meyerdierks, 1999; Shi et al., 2009; Müller et al., 2008, 2015; Kottmeier et al., 2020). Some phytoplankton species grow poorly or not at all under continuous light (Paasche, 1967; Brand and Guillard, 1981), reportedly including the coccolithophore species *Calcidiscus leptoporus* (Brand and Guillard, 1981), the Prymnesiophytes *Isochrysis galbana*, *Chrysochromulina* sp., and the holococcolith form of *Coccolithus pelagicus* (Price et al., 1998). However, several coccolithophore species, including *E. huxleyi*, have been shown to grow well under continuous light (Brand and Guillard, 1981; Price et al., 1998). Additionally, *E. huxleyi* has reportedly been maintained in culture for prolonged periods of time (i.e., several months) under continuous light (Shi et al., 2009; Müller et al., 2017) and several publications explicitly report that the cell cycle of *E. huxleyi* became desynchronised when grown under continuous light (Müller et al., 2008, 2017, 2015, 2012).

We applied continuous light conditions from the onset of our experiments (an abrupt shift from a 12:12 light: dark cycle to continuous light at 0 h) and our 4 h sampling regime enabled the pattern of cell division to be monitored under control, low and high salinity conditions for the duration of each experiment. Unexpectedly, clear cell division phasing persisted under all salinity conditions in both *E. huxleyi* strains for the entire duration of the experiments (>6 days representing 2-4 generations;



Fig. 1 and 2). If the onset of continuous light had desynchronised cell division, we would expect to see \bar{V} stabilise around a constant value and continuously increasing cell concentrations through the course of the experiment (Müller et al. 2015).
395 Instead, we see clear mean cell size minima and maxima in all experiments for both strains corresponding to steplike increases and plateaus in cell concentrations that correspond closely to the timings of the light: dark alternations that preceded the onset of the experiments (Fig. 1). Towards the end of the experiments, declining maximum division rates under salinity 25 and 45 in PLYB11 (Fig. 2) may indicate that phased division of the population was starting to weaken in this strain under low and high salinity stress. However, it is not clear for how many more days phased division might have persisted beyond the end of
400 the experiment. Declining division rates at the end of an experiment may also be an indicator that phased cell division continued but population growth was entering early stationary phase, i.e., growth could no longer proceed exponentially due to one or more changes in the physiochemical conditions of the experiment as cell density increased through the duration of the experiment. Persistent cell cycle phasing for three days after transitioning from a light: dark cycle regime (14:10 L:D) to continuous light has previously been shown for two species of *E. huxleyi* (with a division rate of ca. 1 d^{-1}) as well as the
405 coccolithophore *Chrysothalia carterae* (previously *Hymenomonas carterae*) and three other marine phytoplankton species (Chisholm and Brand, 1981). Cell division phasing of *E. huxleyi* strain CCMP 371 was reportedly desynchronised by “...illumination over several generations with continuous light...” (Müller et al., 2008) but did not further clarify how long this took to achieve. Where publications report the use of continuous light, the pre-experiment acclimation period is stated to be between ca. 7 and 20 generations of growth (Zondervan et al., 2001, 2002; Müller et al., 2008; Bretherton et al., 2019).
410 Assuming that these acclimation periods were sufficient to desynchronise the cell division cycle, we conclude that phasing of cell division to the pre-experiment light: dark conditions in *E. huxleyi* must persist for a minimum of 3-4 generations (as shown by Chisholm and Brand 1981 for populations dividing approximately daily and our experiments with lower growth rates) up to ca. 15 generations or longer. This would equate to 2-3 weeks of growth under experimental conditions for populations dividing with a growth rate of 0.7 d^{-1} and ca. 4-5 weeks for populations dividing with a growth rate of 0.35 d^{-1} . Interestingly,
415 cell cycle entrainment to light: dark cycles may be highly persistent in some strains or in combination with certain environmental stressors, as a previous publication reports culturing *E. huxleyi* for six months under continuous light to ensure complete desynchronisation of the division cycle (Müller et al. 2017).

4.2 Growth and morphological responses to continuous light

Many phytoplankton, including coccolithophores, have higher growth rates under higher irradiance level, longer daylength, or
420 when continuous light is used (e.g., Chisholm and Brand, 1981; Harris et al., 2009; Sheward et al., 2023). We did not measure growth rate before the start of the experiment, so are unable to quantify the impact of the abrupt transition from a 12:12 L:D cycle to continuous light on growth rate under control conditions. However, both strains showed an initial phase of low or negligible increase in cell concentrations over the first ca. 24 h in the control experiment, suggesting that an immediate physiological response to the onset of continuous light probably occurred in all experiments. There are conflicting reports as
425 to whether *E. huxleyi* has higher (Chisholm and Brand, 1981; Price et al., 1998; Bretherton et al., 2019), lower (Van Rijssel



and Gieskes, 2002), or comparable (Zondervan et al., 2001; Rost et al., 2002; Zondervan et al., 2002; Nielsen, 1997) growth rates under continuous light compared to a light: dark regime. The effect of continuous or discontinuous irradiance on *E. huxleyi* growth rate is likely to be strain-specific (Price et al., 1998; Bretherton et al., 2019) and/or vary depending on combination of irradiance level and daylength used (Paasche, 1967; Rost et al., 2002). Subsequently, we cannot rule out that
430 a growth rate response to the abrupt onset of continuous light contributed to growth rate differences between low and high salinity conditions over the course of our experiments. However, we note that Rost et al. (2002) reports that growth rates of the same strain of *E. huxleyi* (PLYB92/11) are comparable under both 16:10 L:D cycle and continuous light when grown under similar irradiance levels (70-100 $\mu\text{mol photons m}^{-2} \text{s}^{-1}$).

In the RCC1232 control experiment, both C_L and \emptyset increase within ca. 28 h of inoculation and then remain at these larger
435 mean values (with some fluctuations) for the remainder of the experiment (Fig. 4b,e). When combined with the overall C_L and \emptyset response to low and high salinity conditions over the course of the experiment, this unexpected increase in C_L and \emptyset under control conditions strongly influences the overall response of C_L and \emptyset across salinities 25, 35 and 45 by 156 h in this strain: C_L increases from salinity 25 to salinity 45 whereas \emptyset is broadly comparable across all salinity treatments as \emptyset increased similarly (Fig. 4). The initial shift in C_L and \emptyset is unlikely to be caused by measurements taken at different points in the cell
440 division cycle (Fig. 1). Instead, the onset of continuous light may have driven a rapid morphological response in RCC1232 that is not observed in PLYB11. Larger cell sizes have previously been reported within 5 h after exposure to higher light conditions for a non-calcifying strain of *E. huxleyi* (Darroch et al., 2015) but in contrast, no significant cell size difference was reported between continuous light and 14:10 L:D experiments for at least one *E. huxleyi* strain (Price et al., 1998).

4.3 Rapid morphological responses to abrupt salinity stress

445 The physiology, cellular composition and gene expression of *E. huxleyi* can rapidly respond to abrupt and short-term (hours to days) changes in carbonate chemistry, light environment, and nutrient levels (e.g., Barcelos E Ramos et al., 2010, 2012; Iglesias-Rodriguez et al., 2017; Darroch et al., 2015). Experiments with other phytoplankton groups have demonstrated that sudden salinity perturbations induce a cascade of rapid metabolic responses within cells, some of which may be coupled with changes in cell size. For example, it only takes seconds to minutes for the green halophilic algae *Dunaliella* to adjust to osmotic
450 differences between the external medium and the cell cytoplasm through rapid, passive water efflux or influx (Weiss and Pick, 1990), which simultaneously drives changes in cell size and volume (Maeda and Thompson, 1986). The impacts of this passive osmotic adjustment on cell size persist for minutes to hours (Weiss and Pick, 1990; Maeda and Thompson, 1986) depending on how rapidly *Dunaliella* restores its ionic equilibrium, e.g., through regulating glycol metabolism (Borowitzka, 2018). To date, the short-term (hours to days) sequence of metabolic responses of *E. huxleyi* under salinity stress remains unknown.
455 Whilst our 4 h sampling frequency is insufficient to capture cell size changes occurring due to turgor pressure adjustment within the first seconds to minutes of exposure to hyposaline (salinity 25) and hypersaline (salinity 45) conditions, as observed

in *Dunaliella*, our experiments do capture rapid changes in *E. huxleyi* growth and morphology over hours to days following the onset of salinity stress.

The timescale of \emptyset and C_L response to abrupt salinity stress (relative to initial strain-specific \emptyset and C_L ; Fig. 3 and 5) was varied and did not show a consistent relationship to strain, salinity treatment or morphological parameter. This is perhaps not surprising, as the response of cell/coccosphere size to salinity in *E. huxleyi* (Saruwatari et al., 2016; Xu et al., 2020b; Gebühr et al., 2021; Hermoso and Lecasble, 2018) and closely related *Gephyrocapsa* species (Hermoso and Lecasble, 2018) seems to be strain-specific (Hermoso and Lecasble, 2018; Gebühr et al., 2021). In addition to differences in the magnitude of cell/coccosphere size response to salinity 25 and 45 conditions between the two strains (Fig. 3-5; Table 1), Norwegian strain PLYB11 generally showed morphological changes after a longer period of exposure (ca. 96-120 h) to salinity 25 and 45 conditions compared to Mediterranean strain RCC1232 (which showed \emptyset changes within 28-36 h).

As cell size responds to the regulation of cell turgor pressure in phytoplankton and other plants (e.g., Kirst, 1990, and references therein), it is plausible that different timescales of morphological response are related to different rates of osmotic adjustment between strains, through osmolyte synthesis, active transport mechanisms, and/or membrane pumps under different salinity conditions. Species-specific synthesis of osmolytes and morphological responses to salinity stress have, for example, been reported for marine diatoms (Helliwell et al., 2021) and references therein) but are currently largely unknown for coccolithophores. *E. huxleyi* is a notable producer of dimethylsulfoniopropionate (DMSP), a compatible solute that contributes to cellular osmotic balance (Kirst, 1996). Cellular concentrations of DMSP are coupled to salinity in many phytoplankton (e.g., Keller and Korjef-Bellows, 1996; Kirst, 1996; Stefels, 2000; Dickson and Kirst, 1987) and in the macroalgae *Ulva* (Van Alstyne et al. 2023). Intracellular concentrations of DMSP have been shown to correlate with salinity in one open-ocean strain of *E. huxleyi* (McParland et al., 2020), *E. huxleyi* strains from a range of environments (Fielding, 2010), and in the coccolithophore species *Gephyrocapsa oceanica* (Larsen and Beardall, 2023) and *Chrysothila carterae* (Vairavamurthy et al., 1985). Cellular DMSP also responds rapidly to some environmental stressors, as quickly as within 4 h under elevated light (Darroch et al. 2015), and the elevated DMSP content of Prymnesiophyceae relative to other phytoplankton groups (Keller et al., 1989; McParland and Levine, 2019) may provide an initial reserve to better tolerate rapid-onset salinity stress (Kirst 1996). However, further investigation is needed to identify the rate of change in cellular ion and osmolyte concentrations for *E. huxleyi* under a range of salinity conditions and strain-specific strategies for osmotic adjustment, as both may impact the capacity of *E. huxleyi* to respond rapidly to the onset of salinity stress.

Changes in C_L with salinity have previously been attributed to changes in the size of the coccolith vesicle proportional to cell volume increase/decreases that occur when water influx/efflux is used to maintain cell turgor pressure (Bollmann et al., 2009; Gebühr et al., 2021). Particularly within short-term experiments as applied here, this hypothesis implies four things: (1) that \emptyset response must precede a C_L response, (2) that the size change of C_L and \emptyset must be positively correlated over some reasonable timeframe (Suchéras-Marx et al., 2022), i.e., cell size does not increase whilst coccolith size decreases or *vice versa*, (3) that the relative magnitude of the cell size change and the corresponding coccolith size change are reasonably proportional (i.e., a small cell size change does not drive a disproportionately large change in coccolith size), and (4) that a change in \emptyset due to one



or more mechanisms to maintain cellular homeostasis must persist for sufficient time for a corresponding increase in C_L to be quantifiable (relative to coccolith production rates).

Overall, our data are broadly consistent with these criteria (Fig. 3 and 5). However, we do see intervals within each experiment where large steplike changes in \emptyset do not correspond proportionally to changes in C_L over the following hours to days (e.g. both strains under salinity 25; Fig. 3 and 5). In some cases (e.g., both strains under salinity 45) were also see \emptyset and C_L changes that occur relatively synchronously (although there is some discrepancy in the C_L and \emptyset sampling timepoints). Generally, changes in C_L tend to emerge more gradually and after a longer period of exposure than changes in \emptyset (Fig. 3 and 5), apart from RCC1232 under salinity 45, where the C_L increases between 24 and 36 h occur within the same timeframe as the \emptyset increase. The measured loose coccoliths initially represent a mix between coccoliths produced during pre-experiment conditions and coccoliths produced under salinity stress, with a diminishing contribution from pre-experiment coccoliths to C_L measurements as the experiment progresses. New coccoliths are produced at least every ca. 60 minutes (Paasche, 2002; Suchéras-Marx et al., 2022) and cells must produce ca. 6-10 new coccoliths between each cell division to ensure a complete cell covering for two daughter cells (based on mean C_N 18-20 in our samples). It would therefore take more than one generation of growth (>24 h when $\mu < 0.7$ d⁻¹) under new environmental conditions before C_L measurements start to reflect the increasing proportion of coccoliths of a different size produced in response to physiological adjustments to the new environment (e.g., salinity). However, coccoliths are produced quickly enough that coccolith size responses should be already evident after two generations, supporting the timescale of morphological responses observed in our 156 h experiment. This might also explain why Iglesias-Rodriguez et al. (2017) did not observed any difference in C_L over a 72-h exposure of *E. huxleyi* strain NZEH to two different low pH deep seawater conditions even though coccosphere volume was significantly different (+30%) between the two deep seawater conditions after 72 h.

4.4 Implications of rapid responses to salinity stress

Whilst our morphological results represent changes over just 2-4 generations of growth under salinity stress, a general pattern of smaller cells with smaller coccoliths under hyposaline conditions (reduced cellular PIC with comparable cellular PIC:POC) and larger cells with larger coccoliths under hypersaline conditions (increased cellular PIC with comparable cellular PIC:POC) emerges from both strains investigated here (Fig. 6; Table 1). A similar pattern of smaller coccoliths under lower salinity and larger coccoliths under higher salinity was also found in acclimated cultures of several different *E. huxleyi* strains, including some open ocean strains (Green et al., 1998; Paasche et al., 1996; Fielding et al., 2009; Linge Johnsen et al., 2019; Saruwatari et al., 2016; Gebühr et al., 2021), in plankton samples (Bollmann et al., 2009), and in sediment core-top samples (Bollmann and Herrle, 2007). The response of coccolith morphology and coccosphere (cell) size to the abrupt change in salinity conditions equates to a rapid (within hours to days) calcification response of *E. huxleyi* to salinity stress, with lower cellular PIC under hyposaline conditions, increased cellular PIC under hypersaline conditions, and similar cellular PIC:POC across all salinity conditions due to the comparable timing of cell (coccosphere) size responses to salinity stress (Table 1). Our results show that



E. huxleyi morphology and calcification is therefore sensitive to even relatively short-term (days to weeks) intervals of abrupt salinity change and, based on evidence from the literature, that these morphological effects are sustained when the new salinity condition persists for weeks to months (as would be typical for experiments using acclimated cultures).

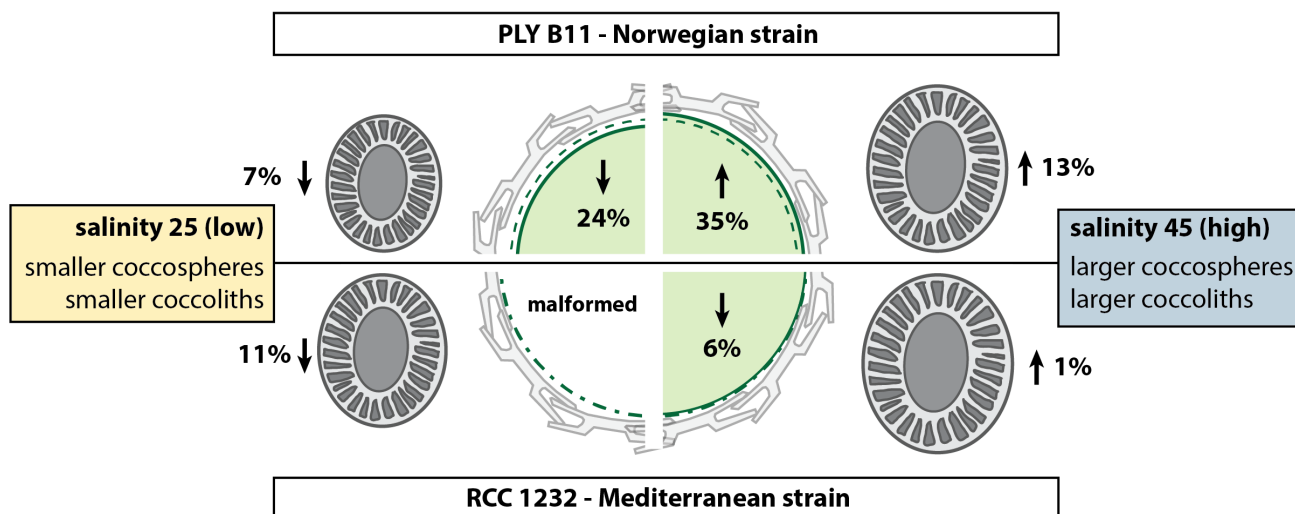


Figure 6: Summary of the morphological response of *E. huxleyi* strains PLYB11 (upper panel) and RCC1232 (lower panel) to abrupt exposure to low salinity 25 conditions (left) and high salinity 45 conditions (right) relative to coccosphere volume (centre cell illustration) and coccolith size (coccolith illustrations) under control salinity 35 conditions. Percentage change values are calculated based on mean C_L and mean \varnothing measurements at 148 h for PLYB11 and 140 h for RCC1232, which represents ca. 6 days growth under the salinity condition (see also Table 1). Dashed green line within the cell illustration indicates equivalent cell size of mean cell volume under salinity 35 conditions at 148 h or 140 h for PLYB11 and RCC1232, respectively.

Changes in coccolith size and coccolith morphology more generally are widely used as proxies for past environmental conditions through time (e.g., Bollmann, 1997; Henderiks and Bollmann, 2004), including paleosalinity (Bollmann et al., 2009; Herrle et al., 2018; Bollmann and Herrle, 2007). The response of *E. huxleyi* coccolith size to salinity stress within hours of exposure in our experiments signifies that transient and extreme salinity events will affect coccolith size in plankton samples alongside longer-term seasonal to decadal salinity trends. Seasonally, calcification responses on such short timeframes may influence surface ocean alkalinity and inorganic carbon export in regions where *E. huxleyi* is a large component of the phytoplankton community. The analysis of coccolith size through time from marine sedimentary records remains most suited to capturing short- to longer-term salinity fluctuations, as sedimentation rates in laminated sediments capture seasonal to annual timescales up to sedimentation rates of thousands to hundreds of thousands of years per cm sediment in deep ocean sediments. However, we emphasise that the rapid morphological response of *E. huxleyi* to salinity (shown here) and other environmental variables, including CO_2 concentrations (Barcelos E Ramos et al., 2010) and exposure to distinct water masses (Iglesias-

Rodriguez et al., 2017), already influence morphology and calcification at a cellular level within only one or two generations of growth. Relative to the timescale of interest, variability in the magnitude and timing of *E. huxleyi* calcification responses to salinity (and likely other environmental parameters) will therefore contribute to the natural within-species variability in morphology and biogeochemical traits observed in natural *E. huxleyi* populations.

550 **Conclusions**

The coccolithophore *E. huxleyi* has a naturally broad salinity tolerance, thriving in both relatively stable open ocean settings and the more variable environmental conditions of shelf-seas and coastal regions. Despite this salinity tolerance, the physiology and morphology of *E. huxleyi* is responsive to changes in salinity. Our experiments show, for the first time, that measurable differences in *E. huxleyi* coccolith size and coccosphere size occur within hours of abrupt exposure to hypo- and hypersaline
555 conditions. The resultant impact of these rapid morphological responses for cellular calcification on short timescales may impact surface ocean carbonate chemistry in regions where *E. huxleyi* is a dominant constituent of phytoplankton communities and contributes to the natural morphological variability of *E. huxleyi* coccoliths in the sedimentary record. The magnitude and timing of the response of *E. huxleyi* to salinity stress is strain-specific and may be related to different osmoregulation capacities between strains, though further exploration of the physiological and biochemical mechanisms underpinning our results was
560 beyond the scope of this study. Further insights would be gained from investigating the magnitude and timing of short-term morphological responses of a broader range of open-ocean and coastal *E. huxleyi* strains to a range of moderate to extreme salinity stress whilst measuring additional physiological indicators (e.g., photophysiology, carbon fixation rates, coccolith geochemistry, and cellular concentrations of DMSP and other solutes). Similarly, it is unclear whether other coccolithophore species respond similarly to the onset of salinity stress, especially as the biogeography of many species is largely restricted to
565 open-ocean settings with a smaller natural salinity range. If trends between morphology and salinity conditions are identified for modern representatives of longer-lived coccolithophore genera, the geological periods over which coccolith morphology can be used as an independent paleosalinity proxy could potentially be extended.

Data availability

All data relating to this study are available at zenodo as Gebühr et al. (2024), doi: 10.5281/zenodo.10610998.

570 **Author contribution**

The study was conceived by JOH, CG, and JB. CG planned and conducted the experiments and data collection. Morphometric data collection was performed by CG and RS. Data analysis and interpretation was performed by RS. The manuscript was written by RS with contributions from all authors.



Competing interests

575 The authors declare that they have no conflict of interest.

Acknowledgments

The authors thank the Roscoff Culture Collection at the Station Biologique in Roscoff, France, and the Plymouth Culture Collection maintained by the Marine Biological Association in Plymouth, UK, for providing the algal strains used in this study. We are grateful to Laboratory Technician Bärbel Schminke for her assistance with culture sampling and scanning electron
580 microscopy. This research was financed by grants awarded to JOH by the State of Hesse (Germany) in the framework of the Initiative for the Development of Scientific and Economic Excellence (LOEWE) the Biodiversity and Climate Centre Frankfurt (BIK-F) grant number R2107 Project PB A, the DAAD-Programm Strategische Partnerschaften of the Goethe-University Frankfurt (grant number UoT6), and the Freunde und Förderer der Goethe-Universität Frankfurt am Main (funding awarded
585 to JOH in 2010). RMS is funded by the Deutsche Forschungsgemeinschaft (DFG, German Research Foundation) project 447581699 and RMS acknowledges additional financial support through the VeWA consortium (*Past Warm Periods as Natural Analogues of our high-CO₂ Climate Future*) by the LOEWE programme of the Hessen Ministry of Higher Education, Research and the Arts, Germany.

References

- Barcelos E Ramos, J., Müller, M. N., and Riebesell, U.: Short-term response of the coccolithophore *Emiliania huxleyi* to an
590 abrupt change in seawater carbon dioxide concentrations, *Biogeosciences*, 7, 177–186, <https://doi.org/10.5194/bg-7-177-2010>, 2010.
- Barcelos E Ramos, J., Schulz, K. G., Febiri, S., and Riebesell, U.: Photoacclimation to abrupt changes in light intensity by *Phaeodactylum tricornerutum* and *Emiliania huxleyi*: The role of calcification, *Mar. Ecol. Prog. Ser.*, 452, 11–26, <https://doi.org/10.3354/meps09606>, 2012.
- 595 Bollmann, J.: Morphology and biogeography of *Gephyrocapsa* coccoliths in Holocene sediments, *Mar. Micropaleontol.*, 29, 319–350, [https://doi.org/10.1016/S0377-8398\(96\)00028-X](https://doi.org/10.1016/S0377-8398(96)00028-X), 1997.
- Bollmann, J. and Herrle, J. O.: Morphological variation of *Emiliania huxleyi* and sea surface salinity, *Earth Planet. Sci. Lett.*, 255, 273–288, <https://doi.org/10.1016/j.epsl.2006.12.029>, 2007.
- Bollmann, J., Herrle, J. O., Cortés, M. Y. Y., and Fielding, S. R.: The effect of sea water salinity on the morphology of
600 *Emiliania huxleyi* in plankton and sediment samples, *Earth Planet. Sci. Lett.*, 284, 320–328, <https://doi.org/10.1016/j.epsl.2009.05.003>, 2009.
- Borowitzka, M. A.: The ‘stress’ concept in microalgal biology - homeostasis, acclimation and adaptation, *J. Appl. Phycol.*, 30, 2815–2825, <https://doi.org/10.1007/s10811-018-1399-0>, 2018.



- Brand, L. E.: The salinity tolerance of forty-six marine phytoplankton isolates, *Estuar. Coast. Shelf Sci.*, 18, 543–556,
605 [https://doi.org/10.1016/0272-7714\(84\)90089-1](https://doi.org/10.1016/0272-7714(84)90089-1), 1984.
- Brand, L. E. and Guillard, R. R. L.: The effects of continuous light and light intensity on the reproduction rates of twenty-two
species of marine phytoplankton, *J. Exp. Mar. Bio. Ecol.*, 50, 119–132, [https://doi.org/10.1016/0022-0981\(81\)90045-9](https://doi.org/10.1016/0022-0981(81)90045-9), 1981.
- Bretherton, L., Poulton, A. J., Lawson, T., Rukminasari, N., Balestreri, C., Schroeder, D., Mark Moore, C., and Suggett, D. J.:
Day length as a key factor moderating the response of coccolithophore growth to elevated $p\text{CO}_2$, *Limnol. Oceanogr.*, 64, 1284–
610 1296, <https://doi.org/10.1002/lno.11115>, 2019.
- Bucciarelli, E., Sunda, W. G., Belviso, S., and Sarthou, G.: Effect of the diel cycle on production of dimethylsulfoniopropionate
in batch cultures of *Emiliania huxleyi*, *Aquat. Microb. Ecol.*, 48, 73–81, <https://doi.org/10.3354/ame048073>, 2007.
- Bukry, D.: Coccoliths as Paleosalinity Indicators - Evidence from the Black Sea, in: *The Black Sea - Geology, Chemistry, and
Biology*, edited by: Degens, E. T. and Ross, D. A., American Association of Petroleum Geologists, Tulsa, OK, USA, 353–
615 363, <https://doi.org/10.1306/M20377C2>, 1974.
- Chisholm, S. W.: Temporal patterns of cell division in unicellular algae, in: *Physiological Bases of Phytoplankton Ecology*,
edited by: Platt, T., *Can B Fish Aquat Sci*, 150–181, 1981.
- Chisholm, S. W. and Brand, L. E.: Persistence of cell division phasing in marine phytoplankton in continuous light after
entrainment to light: dark cycles, *J. Exp. Mar. Bio. Ecol.*, 51, 107–118, [https://doi.org/10.1016/0022-0981\(81\)90123-4](https://doi.org/10.1016/0022-0981(81)90123-4), 1981.
- 620 Darroch, L. J., Lavoie, M., Levasseur, M., Laurion, I., Sunda, W. G., Michaud, S., Scarratt, M., Gosselin, M., and Caron, G.:
Effect of short-term light- and UV-stress on DMSP, DMS, and DMSP lyase activity in *Emiliania huxleyi*, *Aquat. Microb.
Ecol.*, 74, 173–185, <https://doi.org/10.3354/ame01735>, 2015.
- Dickson, D. M. J. and Kirst, G. O.: Osmotic adjustment in marine eukaryotic algae: the role of inorganic ions, quaternary
ammonium, tertiary sulphonium and carbohydrate solutes: I. diatoms and a Rhodophyte, *New Phytol.*, 106, 645–655,
625 <https://doi.org/10.1111/j.1469-8137.1987.tb00165.x>, 1987.
- Durack, P. J. and Wijffels, S. E.: Fifty-Year trends in global ocean salinities and their relationship to broad-scale warming, *J.
Clim.*, 23, 4342–4362, <https://doi.org/10.1175/2010JCLI3377.1>, 2010.
- Durack, P. J., Wijffels, S. E., and Matear, R. J.: Ocean salinities reveal strong global water cycle intensification during 1950
to 2000, *Science*, 336, 455–458, <https://doi.org/10.1126/science.1212222>, 2012.
- 630 Dye, S. R., Berx, B., Opher, J., Tinker, J., and Renshaw, R.: Climate change and salinity of the coastal and marine environment
around the UK, *MCCIP Science Review 2020*, 76–102, <https://doi.org/doi:10.14465/2020.arc04.sal>, 2020.
- Faucher, G., Riebesell, U., and Bach, L. T.: Can morphological features of coccolithophores serve as a reliable proxy to
reconstruct environmental conditions of the past?, *Clim. Past*, 16, 1007–1025, <https://doi.org/10.5194/cp-16-1007-2020>, 2020.
- Fielding, S. R.: *Emiliania huxleyi* cultures as insights into palaeoceanographic proxies and processes, University of Liverpool,
635 UK, 107 pp., 2010.
- Fielding, S. R., Herrle, J. O., Bollmann, J., Worden, R. H., and Montagnes, D. J. S.: Assessing the applicability of *Emiliania
huxleyi* coccolith morphology as a sea-surface salinity proxy, *Limnol. Oceanogr.*, 54, 1475–1480,



- <https://doi.org/10.4319/lo.2009.54.5.1475>, 2009.
- Fisher, N. S. and Honjo, S.: Intraspecific differences in temperature and salinity responses in the coccolithophore *Emiliana huxleyi*, *Biol. Oceanogr.*, 6, 355–361, <https://doi.org/10.1080/01965581.1988.10749537>, 1988.
- 640 Fox-Kemper, B., Hewitt, H. T., Xiao, C., Aðalgeirsdóttir, G., Drijfhout, S. S., Edwards, T. L., Golledge, N. R., Hemer, M., Kopp, R. E., Krinner, G., Mix, A., Notz, D., Nowicki, S., Nurhati, I. S., Ruiz, L., Sallée, J.-B., Slangen, A. B. A., and Yu, Y.: Ocean, Cryosphere and Sea Level Change, in: *Climate Change 2021: The Physical Science Basis. Contribution of Working Group I to the Sixth Assessment Report of the Intergovernmental Panel on Climate Change*, edited by: Masson-Delmotte, V., P., Zhai, A., Pirani, S. L., Connors, P., Péan, C., Berger, S., Caud, N., Chen, Y., Goldfarb, L., Gomis, M. I., Huang, M., Leitzell, K., Lonnoy, E., Matthews, J. B. R., Maycock, T. K., Waterfield, T., Yelekçi, O., Yu, R., and Zhou, B., Cambridge University Press, Cambridge, UK and New York, NY, USA, 1211–1362, <https://doi.org/10.1017/9781009157896.011.1212>, 2021.
- 645 Gebühr, C., Sheward, R. M., Herrle, J. O., and Bollmann, J.: Strain-specific morphological response of the dominant calcifying phytoplankton species *Emiliana huxleyi* to salinity change, *PLoS One*, 16, 1–24, <https://doi.org/10.1371/journal.pone.0246745>, 2021.
- 650 Gebühr, C., Sheward, R. M., and Herrle, J. O.: Growth and morphological measurements of the coccolithophore *Emiliana huxleyi* under three salinity conditions, *Zenodo* [Data set], <https://doi.org/10.5281/zenodo.10610998>, 2024.
- Green, J. C., Heimdal, B. R., Paasche, E., and Moate, R.: Changes in calcification and the dimensions of coccoliths of *Emiliana huxleyi* (Haptophyta) grown at reduced salinities, *Phycologia*, 37, 121–131, <https://doi.org/10.2216/i0031-8884-37-2-121.1>, 1998.
- 655 Guillard, R. R.: Division rates, in: *Handbook of phycological methods: Culture methods and growth measurements*, edited by: Stein, J. R., Cambridge University Press, 289–311, 1973.
- Harding, L. W., Meeson, B. W., Prézelin, B. B., and Sweeney, B. M.: Diel periodicity of photosynthesis in marine phytoplankton, *Mar. Biol.*, 61, 95–105, <https://doi.org/10.1007/BF00386649>, 1981.
- 660 Harris, G. N., Scanlan, D. J., and Geider, R. J.: Responses of *Emiliana huxleyi* (Prymnesiophyceae) to step changes in photon flux density, *Eur. J. Phycol.*, 44, 31–48, <https://doi.org/10.1080/09670260802233460>, 2009.
- Haumann, F. A., Gruber, N., Münnich, M., Frenger, I., and Kern, S.: Sea-ice transport driving Southern Ocean salinity and its recent trends, *Nature*, 537, 89–92, <https://doi.org/10.1038/nature19101>, 2016.
- Helliwell, K. E., Kleiner, F. H., Hardstaff, H., Chrachri, A., Gaikwad, T., Salmon, D., Smirnov, N., Wheeler, G. L., and Brownlee, C.: Spatiotemporal patterns of intracellular Ca^{2+} signalling govern hypo-osmotic stress resilience in marine diatoms, *New Phytol.*, 230, 155–170, <https://doi.org/10.1111/nph.17162>, 2021.
- 665 Henderiks, J. and Bollmann, J.: The *Gephyrocapsa* sea surface palaeothermometer put to the test: comparison with alkenone and foraminifera proxies off NW Africa, *Mar. Micropaleontol.*, 50, 161–184, [https://doi.org/10.1016/S0377-8398\(03\)00070-7](https://doi.org/10.1016/S0377-8398(03)00070-7), 2004.
- 670 Hermoso, M. and Lécasle, M.: The effect of salinity on the biogeochemistry of the coccolithophores with implications for coccolith-based isotopic proxies, *Biogeosciences*, 15, 6761–6772, <https://doi.org/10.5194/bg-15-6761-2018>, 2018.



- Herrle, J. O., Bollmann, J., Gebühr, C., Schulz, H., Sheward, R. M., and Giesenberg, A.: Black Sea outflow response to Holocene meltwater events, *Sci. Rep.*, 8, 4081, <https://doi.org/10.1038/s41598-018-22453-z>, 2018.
- Holligan, P. M., Fermindez, E., Balch, W. M., Boyd, P., Peter, H., Finch, M., Groom, B., Muller, K., Putdie, D. A., Trees, C., Turner, S. M., Kingdom, U., Diego, S., and Diego, S.: A biogeochemical study of the coccolithophore, *Emiliana huxleyi*, in the North Atlantic, *Global Biogeochem. Cycles*, 7, 879–900, 1993.
- Iglesias-Rodriguez, M. D., Jones, B. M., Blanco-Ameijeiras, S., Greaves, M., Huete-Ortega, M., and Lebrato, M.: Physiological responses of coccolithophores to abrupt exposure of naturally low pH deep seawater, *PLoS One*, 12, 1–20, <https://doi.org/10.1371/journal.pone.0181713>, 2017.
- 680 Jochem, F. J. and Meyerdierks, D.: Cytometric measurement of the DNA cell cycle in the presence of chlorophyll autofluorescence in marine eukaryotic phytoplankton by the blue-light excited dye YOYO-1, *Mar. Ecol. Prog. Ser.*, 185, 301–307, <https://doi.org/10.3354/meps185301>, 1999.
- Kapsenberg, L., Alliouane, S., Gazeau, F., Mousseau, L., and Gattuso, J. P.: Coastal ocean acidification and increasing total alkalinity in the northwestern Mediterranean Sea, *Ocean Sci.*, 13, 411–426, <https://doi.org/10.5194/os-13-411-2017>, 2017.
- 685 Keller, M. D. and Korjef-Bellows, W.: Physiological aspects of the production of dimethylsulfoniopropionate (DMSP) by marine phytoplankton, in: *Biological and Environmental Chemistry of DMSP and Related Sulfonium Compounds*, edited by: Kiene, R. P. et al., Plenum Press, New York, 131–142, https://doi.org/10.1007/978-1-4613-0377-0_12, 1996.
- Keller, M. D., Bellows, W. K., and Guillard, R. R. L.: Dimethyl Sulfide Production in Marine Phytoplankton, in: *Biogenic Sulfur in the Environment*, edited by: Saltzman, E. et al., American Chemical Society, Washington DC, 167–182, <https://doi.org/10.1021/bk-1989-0393.ch011>, 1989.
- 690 Kirst, G.: Osmotic adjustment in the phytoplankton: The use of dimethylsulfoniopropionate (DMSP), in: *Biological and Environmental Chemistry of DMSP and Related Sulfonium Compounds*, edited by: Kiene, R. P., Plenum Press, New York, 121–129, 1996.
- Kirst, G. O.: Salinity tolerance of eukaryotic marine algae, *Annu. Rev. Plant Physiol. Plant Mol. Biol.*, 41, 21–53, <https://doi.org/10.1146/annurev.pp.41.060190.000321>, 1990.
- 695 Kottmeier, D. M., Terbrüggen, A., Wolf-Gladrow, D. A., and Thoms, S.: Diel variations in cell division and biomass production of *Emiliana huxleyi*—Consequences for the calculation of physiological cell parameters, *Limnol. Oceanogr.*, 1–20, <https://doi.org/10.1002/lno.11418>, 2020.
- Lamoureux, S. F. and Bollmann, J.: Image Analysis, in: *Image Analysis, Sediments and Paleoenvironments*, edited by: Francus, P., Kluwer Academic Publishers, Dordrecht, The Netherlands, 330, <https://doi.org/10.1007/1-4020-2122-4>, 2004.
- 700 Larsen, S. H. and Beardall, J.: The effect of temperature and salinity on DMSP production in *Gephyrocapsa oceanica* (Isochrysidales, Coccolithophyceae), *Phycologia*, 62, 152–163, <https://doi.org/10.1080/00318884.2023.2170636>, 2023.
- Lenderink, G. and Van Meijgaard, E.: Increase in hourly precipitation extremes beyond expectations from temperature changes, *Nat. Geosci.*, 1, 511–514, <https://doi.org/10.1038/ngeo262>, 2008.
- 705 Linge Johnsen, S. A., Bollmann, J., Gebuehr, C., and Herrle, J. O.: Relationship between coccolith length and thickness in the



- coccolithophore species *Emiliana huxleyi* and *Gephyrocapsa oceanica*, PLoS One, 14, 1–23, <https://doi.org/10.1371/journal.pone.0220725>, 2019.
- Liu, H., Xu, T., Li, D., Nie, X., and Wei, Z.: Sea surface salinity extremes over the global ocean, Environ. Res. Lett., 18, <https://doi.org/10.1088/1748-9326/ad0165>, 2023.
- 710 Lohbeck, K. T., Riebesell, U., Collins, S., and Reusch, T. B. H.: Functional genetic divergence in high CO₂ adapted *Emiliana huxleyi* populations, Evolution (N. Y.), 67, 1892–1900, <https://doi.org/10.1111/j.1558-5646.2012.01812.x>, 2013.
- Maeda, M. and Thompson, G. A.: On the mechanism of rapid plasma membrane and chloroplast envelope expansion in *Dunaliella salina* exposed to hypoosmotic shock., J. Cell Biol., 102, 289–297, <https://doi.org/10.1083/jcb.102.1.289>, 1986.
- McParland, E. L. and Levine, N. M.: The role of differential DMSP production and community composition in predicting variability of global surface DMSP concentrations, Limnol. Oceanogr., 64, 757–773, <https://doi.org/10.1002/lno.11076>, 2019.
- 715 McParland, E. L., Wright, A., Art, K., He, M., and Levine, N. M.: Evidence for contrasting roles of dimethylsulfoniopropionate production in *Emiliana huxleyi* and *Thalassiosira oceanica*, New Phytol., 226, 396–409, <https://doi.org/10.1111/nph.16374>, 2020.
- Menden-Deuer, S. and Lessard, E. J.: Carbon to volume relationships for dinoflagellates, diatoms, and other protist plankton, Limnol. Oceanogr., 45, 569–579, <https://doi.org/10.4319/lo.2000.45.3.0569>, 2000.
- 720 Müller, M. N., Antia, A. N., and LaRoche, J.: Influence of cell cycle phase on calcification in the coccolithophore *Emiliana huxleyi*, Limnol. Oceanogr., 53, 506–512, 2008.
- Müller, M. N., Beaufort, L., Bernard, O., Pedrotti, M. L., Talec, A., and Sciandra, A.: Influence of CO₂ and nitrogen limitation on the coccolith volume of *Emiliana huxleyi* (Haptophyta), Biogeosciences, 9, 4155–4167, <https://doi.org/10.5194/bg-9-4155-2012>, 2012.
- 725 Müller, M. N., Trull, T. W., and Hallegraeff, G. M.: Differing responses of three Southern Ocean *Emiliana huxleyi* ecotypes to changing seawater carbonate chemistry, Mar. Ecol. Prog. Ser., 531, 81–90, <https://doi.org/10.3354/meps11309>, 2015.
- Müller, M. N., Trull, T. W., and Hallegraeff, G. M.: Independence of nutrient limitation and carbon dioxide impacts on the Southern Ocean coccolithophore *Emiliana huxleyi*, ISME J., 1–11, <https://doi.org/10.1038/ismej.2017.53>, 2017.
- 730 Nederbragt, A. J., Francus, P., Bollmann, J., and Soreghan, M. J.: Image calibration, filtering, and processing, in: Image Analysis, Sediments and Paleoenvironments, edited by: Francus, P., Kluwer Academic Publishers, Dordrecht, The Netherlands, 330, <https://doi.org/10.1007/1-4020-2122-4>, 2004.
- Nelson, D. and Brand, L.: Cell division periodicity in 13 species of marine phytoplankton on a light:dark cycle, J. Phycol., 15, 67–75, 1979.
- 735 Nielsen, M. V.: Growth, dark respiration and photosynthetic parameters of the coccolithophorid *Emiliana huxleyi* (Prymnesiophyceae) acclimated to different day length-irradiance combinations, J. Phycol., 33, 818–822, 1997.
- Paasche, E.: Marine plankton algae grown with light-dark cycles. I. *Coccolithus huxleyi*, Physiol. Plant., 20, 946–956, <https://doi.org/10.1111/j.1399-3054.1967.tb08382.x>, 1967.
- Paasche, E.: A review of the coccolithophorid *Emiliana huxleyi* (Prymnesiophyceae), with particular reference to growth,



- 740 coccolith formation, and calcification-photosynthesis interactions, *Phycologia*, 40, 503–529, <https://doi.org/10.2216/i0031-8884-40-6-503.1>, 2002.
- Paasche, E., Brubak, S., Skattebol, S., Young, J. R., and Green, J. C.: Growth and calcification in the coccolithophorid *Emiliana huxleyi* (Haptophyceae) at low salinities, *Phycologia*, 35, 394–403, <https://doi.org/10.2216/i0031-8884-35-5-394.1>, 1996.
- 745 Paulino, A. I., Larsen, A., Bratbak, G., Evens, D., Erga, S. R., Bye-Ingebrigtsen, E., and Egge, J. K.: Seasonal and annual variability in the phytoplankton community of the Raunefjord, west coast of Norway from 2001–2006, *Mar. Biol. Res.*, 14, 421–435, <https://doi.org/10.1080/17451000.2018.1426863>, 2018.
- Poppeschi, C., Charria, G., Goberville, E., Rimmelin-Maury, P., Barrier, N., Petton, S., Unterberger, M., Grossteffan, E., Repecaud, M., Quémener, L., Theetten, S., Le Roux, J. F., and Tréguer, P.: Unraveling salinity extreme events in coastal environments: A winter focus on the Bay of Brest, *Front. Mar. Sci.*, 8, <https://doi.org/10.3389/fmars.2021.705403>, 2021.
- 750 Poulton, A. J., Painter, S. C., Young, J. R., Bates, N. R., Bowler, B., Drapeau, D., Lyczsekowski, E., and Balch, W. M.: The 2008 *Emiliana huxleyi* bloom along the Patagonian Shelf: Ecology, biogeochemistry, and cellular calcification, *Global Biogeochem. Cycles*, 27, 1023–1033, 2013.
- Poulton, A. J., Stinchcombe, M. C., Achterberg, E. P., Bakker, D. C. E., Dumousseaud, C., Lawson, H. E., Lee, G. A., Richier, S., Suggett, D. J., and Young, J. R.: Coccolithophores on the north-west European shelf: Calcification rates and environmental controls, *Biogeosciences*, 11, 3919–3940, <https://doi.org/10.5194/bg-11-3919-2014>, 2014.
- 755 Price, L. L., Yin, K., and Harrison, P. J.: Influence of continuous light and L:D cycles on the growth and chemical composition of Prymnesiophyceae including coccolithophores, *J. Exp. Mar. Bio. Ecol.*, 223, 223–234, [https://doi.org/10.1016/S0022-0981\(97\)00168-8](https://doi.org/10.1016/S0022-0981(97)00168-8), 1998.
- 760 Van Rijssel, M. and Gieskes, W. W. C.: Temperature, light, and the dimethylsulfoniopropionate (DMSP) content of *Emiliana huxleyi* (Prymnesiophyceae), *J. Sea Res.*, 48, 17–27, [https://doi.org/10.1016/S1385-1101\(02\)00134-X](https://doi.org/10.1016/S1385-1101(02)00134-X), 2002.
- Rost, B., Zondervan, I., and Riebesell, U.: Light-dependent carbon isotope fractionation in the coccolithophorid *Emiliana huxleyi*, *Limnol. Oceanogr.*, 47, 120–128, <https://doi.org/10.4319/lo.2002.47.1.0120>, 2002.
- Röthig, T., Trevathan-Tackett, S. M., Voolstra, C. R., Ross, C., Chaffron, S., Durack, P. J., Warmuth, L. M., and Sweet, M.: Human-induced salinity changes impact marine organisms and ecosystems, *Glob. Chang. Biol.*, 4731–4749, <https://doi.org/10.1111/gcb.16859>, 2023.
- 765 Saruwatari, K., Satoh, M., Harada, N., Suzuki, I., and Shiraiwa, Y.: Change in coccolith morphology by responding to temperature and salinity in coccolithophore *Emiliana huxleyi* (Haptophyta) isolated from the Bering and Chukchi Seas, *Biogeosciences*, 13, 2743–2755, <https://doi.org/10.5194/bgd-12-17751-2015>, 2016.
- 770 Sheward, R. M., Liefer, J. D., Irwin, A. J., and Finkel, Z. V.: Elemental stoichiometry of the key calcifying marine phytoplankton *Emiliana huxleyi* under ocean climate change: A meta-analysis, *Glob. Chang. Biol.*, 29, 4259–4278, <https://doi.org/10.1111/gcb.16807>, 2023.
- Shi, D., Xu, Y., and Morel, F. M. M.: Effects of the pH/pCO₂ control method on medium chemistry and phytoplankton growth,



- Biogeosciences, 6, 1199–1207, <https://doi.org/10.5194/bg-6-1199-2009>, 2009.
- 775 Stefels, J.: Physiological aspects of the production and conversion of DMSP in marine algae and higher plants, *J. Sea Res.*, 43, 183–197, [https://doi.org/10.1016/S1385-1101\(00\)00030-7](https://doi.org/10.1016/S1385-1101(00)00030-7), 2000.
- Suchéras-Marx, B., Viseur, S., Walker, C. E., Beaufort, L., Probert, I., and Bolton, C.: Coccolith size rules – What controls the size of coccoliths during coccolithogenesis?, *Mar. Micropaleontol.*, 170, 102080, <https://doi.org/10.1016/j.marmicro.2021.102080>, 2022.
- 780 Tyrrell, T. and Merico, A.: *Emiliana huxleyi*: bloom observation and the conditions that induce them, in: *Coccolithophores: From Molecular Processes to Global Impact*, edited by: Thierstein, H. R. and Young, J. R., Springer, Berlin, 585–604, 2004.
- Vairavamurthy, A., Andreae, M. O., and Iverson, R. L.: Biosynthesis of dimethylsulfide and dimethylpropiothetin by *Hymenomonas carterae* in relation to sulfur source and salinity variations, *Limnol. Oceanogr.*, 30, 59–70, <https://doi.org/10.4319/lo.1985.30.1.0059>, 1985.
- 785 Van Der Wal, P., Kempers, R. S., and Veldhuis, M. J. W.: Production and downward flux of organic matter and calcite in a North Sea bloom of the coccolithophore *Emiliana huxleyi*, *Mar. Ecol. Prog. Ser.*, 126, 247–265, <https://doi.org/10.3354/meps126247>, 1995.
- Weiss, M. and Pick, U.: Transient Na⁺ flux following hyperosmotic shock in the halotolerant alga *Dunaliella salina*: a response to intracellular pH changes, *J. Plant Physiol.*, 136, 429–438, [https://doi.org/10.1016/S0176-1617\(11\)80031-3](https://doi.org/10.1016/S0176-1617(11)80031-3), 1990.
- 790 Westra, S., Fowler, H. J., Evans, J. P., Alexander, L. V., Berg, P., Johnson, F., Kendon, E. J., Lenderink, G., and Roberts, N. M.: Future changes to the intensity and frequency of short-duration extreme rainfall, *Rev. Geophys.*, 52, 522–555, <https://doi.org/10.1002/2014RG000464>, 2014.
- Winter, A., Reiss, Z., and Luz, B.: Distribution of living coccolithophore assemblages in the Gulf of Elat ('Aqaba), *Mar. Micropaleontol.*, 4, 197–223, [https://doi.org/10.1016/0377-8398\(79\)90017-3](https://doi.org/10.1016/0377-8398(79)90017-3), 1979.
- 795 Winter, A., Henderiks, J., Beaufort, L., Rickaby, R. E. M., and Brown, C. W.: Poleward expansion of the coccolithophore *Emiliana huxleyi*, *J. Plankton Res.*, 0, 1–10, <https://doi.org/10.1093/plankt/fbt110>, 2013.
- Wood, A. M., Everroad, R. C., and Wingard, L. M.: Measuring growth rates in microalgal cultures, in: *Algal Culturing Techniques*, edited by: Andersen, R. A., Elsevier Academic Press, Oxford, 269–286, 2005.
- Xu, H., Yu, R., Liu, Y., Tang, D., Wang, S., and Fu, D.: Effects of tropical cyclones on sea surface salinity in the Bay of Bengal based on SMAP and Argo data, *Water*, 12, 2975, <https://doi.org/10.3390/w12112975>, 2020a.
- 800 Xu, J., Sun, J., Beardall, J., and Gao, K.: Lower salinity leads to improved physiological performance in the coccolithophorid *Emiliana huxleyi*, which partly ameliorates the effects of ocean acidification, *Front. Mar. Sci.*, 7, 1–18, <https://doi.org/10.3389/fmars.2020.00704>, 2020b.
- Young, J. R. and Ziveri, P.: Calculation of coccolith volume and its use in calibration of carbonate flux estimates, *Deep Sea Res. Part II Top. Stud. Oceanogr.*, 47, 1679–1700, [https://doi.org/10.1016/S0967-0645\(00\)00003-5](https://doi.org/10.1016/S0967-0645(00)00003-5), 2000.
- 805 Yu, L., Bingham, F. M., Lee, T., Dinnat, E. P., Fournier, S., Melnichenko, O., Tang, W., and Yueh, S. H.: Revisiting the global patterns of seasonal cycle in sea surface salinity, *J. Geophys. Res. Ocean.*, 126, 1–27, <https://doi.org/10.1029/2020JC016789>,



2021.

810 Zondervan, I., Zeebe, R. E., Rost, B., and Riebesell, U.: Decreasing marine biogenic calcification: a negative feedback on rising atmospheric pCO₂, *Global Biogeochem. Cycles*, 15, 507–516, 2001.

Zondervan, I., Rost, B., and Riebesell, U.: Effect of CO₂ concentration on the PIC/POC ratio in the coccolithophore *Emiliana huxleyi* grown under light-limiting conditions and different daylengths, *J. Exp. Mar. Bio. Ecol.*, 272, 55–70, [https://doi.org/10.1016/S0022-0981\(02\)00037-0](https://doi.org/10.1016/S0022-0981(02)00037-0), 2002.